

Algorithms for Density, Potential Temperature, Conservative Temperature, and the Freezing Temperature of Seawater

DAVID R. JACKETT AND TREVOR J. MCDUGALL

CSIRO Marine and Atmospheric Research, Hobart, Tasmania, Australia

RAINER FEISTEL

Institut für Ostseeforschung, Warnemünde, Germany

DANIEL G. WRIGHT

Department of Fisheries and Oceans, Bedford Institute of Oceanography, Dartmouth, Nova Scotia, Canada

STEPHEN M. GRIFFIES

NOAA/Geophysical Fluid Dynamics Laboratory, Princeton, New Jersey

(Manuscript received 8 July 2005, in final form 30 March 2006)

ABSTRACT

Algorithms are presented for density, potential temperature, conservative temperature, and the freezing temperature of seawater. The algorithms for potential temperature and density (in terms of potential temperature) are updates to routines recently published by McDougall et al., while the algorithms involving conservative temperature and the freezing temperatures of seawater are new. The McDougall et al. algorithms were based on the thermodynamic potential of Feistel and Hagen; the algorithms in this study are all based on the “new extended Gibbs thermodynamic potential of seawater” of Feistel. The algorithm for the computation of density in terms of salinity, pressure, and conservative temperature produces errors in density and in the corresponding thermal expansion coefficient of the same order as errors for the density equation using potential temperature, both being twice as accurate as the International Equation of State when compared with Feistel’s new equation of state. An inverse function relating potential temperature to conservative temperature is also provided. The difference between practical salinity and absolute salinity is discussed, and it is shown that the present practice of essentially ignoring the difference between these two different salinities is unlikely to cause significant errors in ocean models.

1. Introduction

McDougall et al. (2003, hereafter MJWF03) have recently fitted a 25-term rational function to seawater density, when considered a function of salinity S , potential temperature θ , and pressure p . The major motivation for the development of this equation of state was that ocean models have been cast in terms of potential temperature (rather than in situ temperature) as their ocean temperature variable, and an accurate and effi-

cient code for the computation of density in these terms was lacking. The 25-term equation was also motivated by publication of the Feistel and Hagen (1995, hereafter FH95) equation of state, which was based on a Gibbs thermodynamic potential. This equation turned out to be more accurate than, and addressed several weaknesses in, the well-established International Equation of State of Seawater (Fofonoff and Millard 1983). MJWF03 also presented a new algorithm for the computation of potential temperature that was thermodynamically consistent with the FH95 ocean density routine. The algorithms they presented resulted in a code that was substantially more efficient for computing density and potential temperature than routines based on the power series representation of the Gibbs potential,

Corresponding author address: Dr. David R. Jackett, CSIRO Marine and Atmospheric Research, GPO Box 1538, Hobart, TAS 7001, Australia.
E-mail: david.jackett@csiro.au

and achieved an accuracy for the important oceanographic variables of the same order as the accuracy of the Feistel and Hagen fits compared with the then most recently available ocean data.

More recently, Feistel (2003, hereafter F03) has updated the Gibbs potential by both the inclusion of new data constraints and the addition of higher-order terms in its power series representation. Complete details of all the improvements can be found in F03, but here we mention the recalibration of old seawater data for compatibility with the 1995 international scientific pure water standard (IAPWS-95: Wagner and Pruß 2002) and inclusion of the triple point of water in the fit of the Gibbs function. This has led to better sound speed estimates at high pressures. Temperatures of maximum density are reproduced to the accuracy of the experimental data. The accuracy in fitting real ocean data has also been improved over that in FH95 by increasing by one the powers of temperature, salinity, and pressure in the power series expression for the Gibbs potential. This leads to a potential function with 101 coefficients, resulting in more than a 20% increase in computational cost over the 83-term power series of FH95.

Given these improvements in the Gibbs thermodynamic potential together with its increased computational cost, a refit of the functions underlying the algorithms of MJWF03 seemed in order. Again, we have chosen rational functions as our fundamental fitting functions, owing to the rich and stable nature such functional representations provide. Although we could have changed various terms in the 25-term rational function approximation to density $\rho(S, \theta, p)$, we have chosen to retain the same terms for consistency with the corresponding routines in MJWF03 and for ease of implementation in current ocean models. Although the number of terms in the Gibbs potential has been increased, we find that the original form of our rational function approximation leads to fits with errors for key oceanographic variables of the same order as the corresponding errors of the Gibbs function fit of F03 to the underlying thermodynamic data. We show that these errors are approximately one-half of those arising from the spatial variability in the composition of seawater (Millero 2000).

The thermodynamic variable whose advection and diffusion most accurately represents the first law of thermodynamics is potential enthalpy (McDougall 2003), a variable easily computed from the Gibbs potential of either FH95 or F03, and it is convenient to form a new temperature variable, called conservative temperature, by simply dividing potential enthalpy by a fixed value of heat capacity. Complete details of the theoretical justification for and the properties of this

conservative temperature variable can be found in McDougall (2003). Since ocean models treat their temperature variable as conservative, it is more appropriate to interpret ocean model temperature as conservative temperature rather than the present practice, which is to interpret the model's temperature as potential temperature. To run ocean models with this temperature variable, an equation of state is needed that is a function of conservative temperature, salinity, and pressure, and we here present such an equation. Also, an algorithm is presented for the calculation of potential temperature in terms of salinity and conservative temperature so that, for example, sea surface temperature can be calculated from an ocean model's internal conservative temperature.

We also include a simple rational function for the freezing point of seawater that is based on the new F03 Gibbs thermodynamic potential in combination with the new Gibbs function of ice (Feistel and Wagner 2005, hereafter FW05). Throughout we use the symbols T , θ , and Θ to represent the three temperature variables: in situ temperature, potential temperature, and conservative temperature—in degrees Celsius. Salinity, as usually measured and based on conductivity measurements, is denoted by S and absolute salinity, the mass of salt per mass of seawater (in grams per kilogram), is given the symbol S_A . Pressure is denoted by p , density by ρ , and the reference pressure to which potential variables are referred is p_r . All temperature variables are based on in situ temperature being measured in °C on the 1990 International Temperature Scale (ITS-90: Preston-Thomas 1990), pressures are in decibars (1 dbar = 10^4 Pa), and salinity is expressed on the Practical Salinity Scale 1978 (PSS-78: Lewis and Perkin 1981). All pressures are gauge pressures; that is, they are the absolute pressures less 10.1325 dbar.

In section 2 we update the algorithms found in MJWF03, while section 3 contains three algorithms associated with conservative temperature: the forward function, an equation of state, and an inverse function. Section 4 then deals with freezing temperature formulas for in situ temperature, conservative temperature, and potential temperature. In section 5 we discuss the differences between absolute and practical salinity in ocean models, and section 6 concludes the paper.

2. Updated algorithms for potential temperature $\theta(S, T, p, p_r)$ and the $\rho(S, \theta, p)$ equation of state

Here we update the two algorithms appearing in MJWF03.

a. Potential temperature $\theta(S, T, p, p_r)$

The routine for calculating the potential temperature of seawater is identical to the corresponding algorithm in MJWF04, and the updated coefficients can be found in section a of appendix A. We test the accuracy of the new values of θ by examining the root-mean-square (rms) and maximum absolute errors when 10^6 random fluid parcels (S - T - p), drawn from the cube $[0, 42 \text{ psu}] \times [-2^\circ\text{C}, 40^\circ\text{C}] \times [0 \text{ dbar}, 10^4 \text{ dbar}]$, are referenced to another 10^6 random pressures in the range $[0 \text{ dbar}, 10^4 \text{ dbar}]$. The potential temperatures against which we compare the estimates of θ are those obtained by iterating the standard Newton–Raphson technique from the in situ temperatures to their fixed points (see section a of appendix A). The accuracy of the recommended two iterations of the algorithm of the first subsection of appendix A is $2.84 \times 10^{-14} \text{ }^\circ\text{C}$ (maximum absolute) and $3.50 \times 10^{-15} \text{ }^\circ\text{C}$ (rms), respectively, effectively being machine precision. In terms of efficiency, the algorithm presented here for the computation of θ is 3.5 times faster than the computation of θ by iteration from T to the potential temperature fixed point.

The maximum difference between potential temperature (referenced to 0 dbar) determined from the entropy of FH95 (as in MJWF03) and the entropy of F03 (as in this paper) for the ocean atlas data of Koltermann et al. (2004; see also Gouretski and Koltermann 2004) is 3 mK, which is very similar to the difference (2.5 mK) between θ determined by the Fofonoff and Millard (1983) algorithm and that of MJWF03, as reported in that paper. Also, as discussed in MJWF03, an uncertainty in the thermal expansion coefficient of $6 \times 10^{-7} \text{ }^\circ\text{C}^{-1}$ leads to a maximum uncertainty in $\theta - T$ of 2 mK for a pressure difference of 5000 dbar. We conclude that in the oceanographic range of variables, each of the three algorithms for θ (i.e., Fofonoff and Millard 1983, MJWF03, and the present paper) differ from each other by approximately the same amount. Nevertheless, the present approach is preferable for the calculation of θ since it uses the most accurate Gibbs function that is available to date and so is likely to be the most accurate of the three methods.

b. The $\rho(S, \theta, p)$ equation of state

Coefficients of the new $\rho(S, \theta, p)$ equation of state are given in section a of appendix A. To test the accuracy of the new equation, uniformly distributed (S, T, p) points were taken from a “funnel” of data, very similar to but slightly larger than the funnel used in the corresponding fit in MJWF03. At the sea surface the minimum in situ temperature is taken to be 2°C below the in situ temperature at which seawater freezes at a pres-

sure of 500 dbar, and the maximum temperature is 40°C , while salinity varies from 0 to 42. The minimum temperature limit and the maximum salinity limit are independent of pressure. The maximum temperature limit and the lower salinity limit are varied as linear functions of pressure so that the upper temperature bound is 15°C , while the minimum salinity is 30 psu at 5500 dbar. Below this pressure, temperature and salinity extremes are held constant all the way down to 8500 dbar. While this funnel is used to set the range of values used in the fitting exercise, a slightly narrower and shallower funnel [from the freezing temperature (at 500 dbar) up to 33°C at the sea surface and up to 12°C at 5500–8000 dbar] is used to report the errors of the fit. A three-dimensional view of this latter funnel is shown in Fig. 1a while cross sections of the funnel are plotted as solid lines in Figs. 1b and 1c. The freezing temperature plotted in Fig. 1c corresponds to a salinity value of 35 psu. Also plotted in Figs. 1b and 1c are the extremes of the Koltermann et al. (2004) climatology (dashed lines) to indicate how real ocean data fits inside the narrower error funnel.

Figure 2 shows the errors in (a) density $\rho(S, \theta, p)$ (Fig. 2a), (b) the thermal expansion coefficient $\alpha = -\rho^{-1} \partial\rho/\partial\theta|_{S,p}$, (c) the haline contraction coefficient $\beta = \rho^{-1} \partial\rho/\partial S|_{\theta,p}$, (d) sound speed from $(c_s)^{-2} = \partial\rho/\partial p|_{S,\theta}$; all are plotted as functions of pressure. The solid lines in Fig. 2 show rms and maximum absolute differences between these four variables and corresponding quantities computed directly from the in situ density function of F03. Also shown in each panel as dashed lines are the rms and maximum absolute errors for data taken from the Koltermann et al. (2004) isopycnally averaged World Ocean climatology. The errors in α and β should be compared with typical ocean atlas values that are of order $1.5 \times 10^{-4} \text{ K}^{-1}$ and $7.5 \times 10^{-4} (\text{psu})^{-1}$, respectively. [While salinity measured on the Practical Salinity Scale does not strictly have a “unit,” there are many occasions where one needs to be specific about the type of salinity that is used (e.g., whether the practical salinity scale is used or whether salinity is expressed in kg kg^{-1} or g kg^{-1}), and in these situations we use the “psu” nomenclature.]

When compared with the corresponding figure of MJWF03 (their Fig. 3), funnel errors in all the variables here are 20%–160% larger than the corresponding errors in MJWF03. These errors could be lowered by the inclusion of more terms in the rational function or by exchanging terms in the 25-term rational function with terms involving other powers of S , θ , and p . The latter possibility was examined and resulted in only minor improvements. However, the errors in Fig. 2 are already of the same order as errors in the power series fit

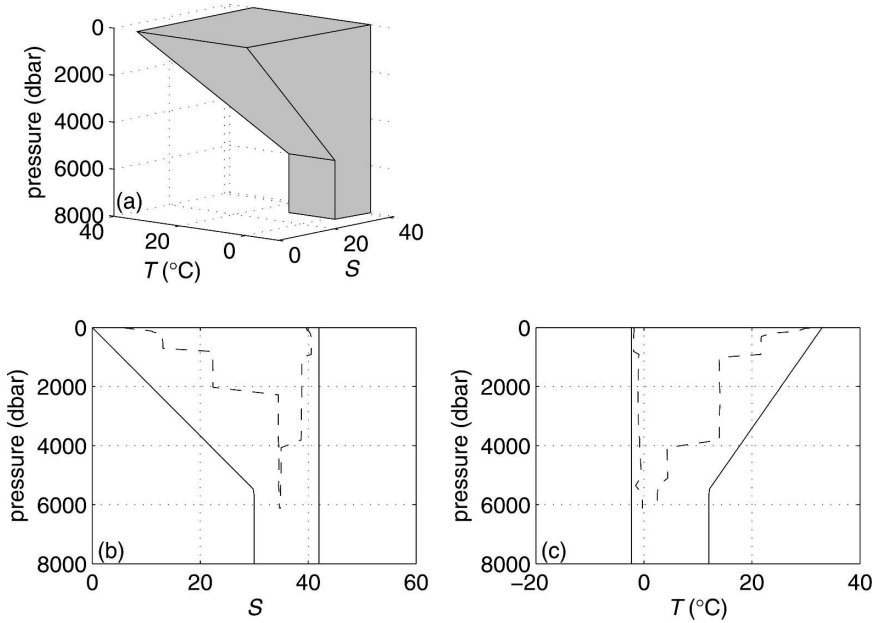


FIG. 1. (a) A three-dimensional view and (b), (c) cross sections of the funnel over which the error in the fit of our 25-term equation was evaluated. Dashed lines in (b) and (c) represent extreme values of data taken from the Koltermann et al. (2004) climatology.

of the Gibbs function in F03 to the underlying data, so we decided that a change in functional form was not warranted. For example, Table 9 of F03 indicates that rms errors as large as $10^{-2} \text{ kg m}^{-3}$ in density and $7.3 \times 10^{-7} \text{ K}^{-1}$ in the thermal expansion coefficient are

present in the F03 fit. The rms errors in the data underlying the F03 fits are $3 \times 10^{-2} \text{ kg m}^{-3}$ for density and $6.0 \times 10^{-7} \text{ K}^{-1}$ for the thermal expansion coefficient. The errors in density shown in Fig. 2 are $2.4 \times 10^{-3} \text{ kg m}^{-3}$ (rms) and $6.5 \times 10^{-3} \text{ kg m}^{-3}$ (max), and

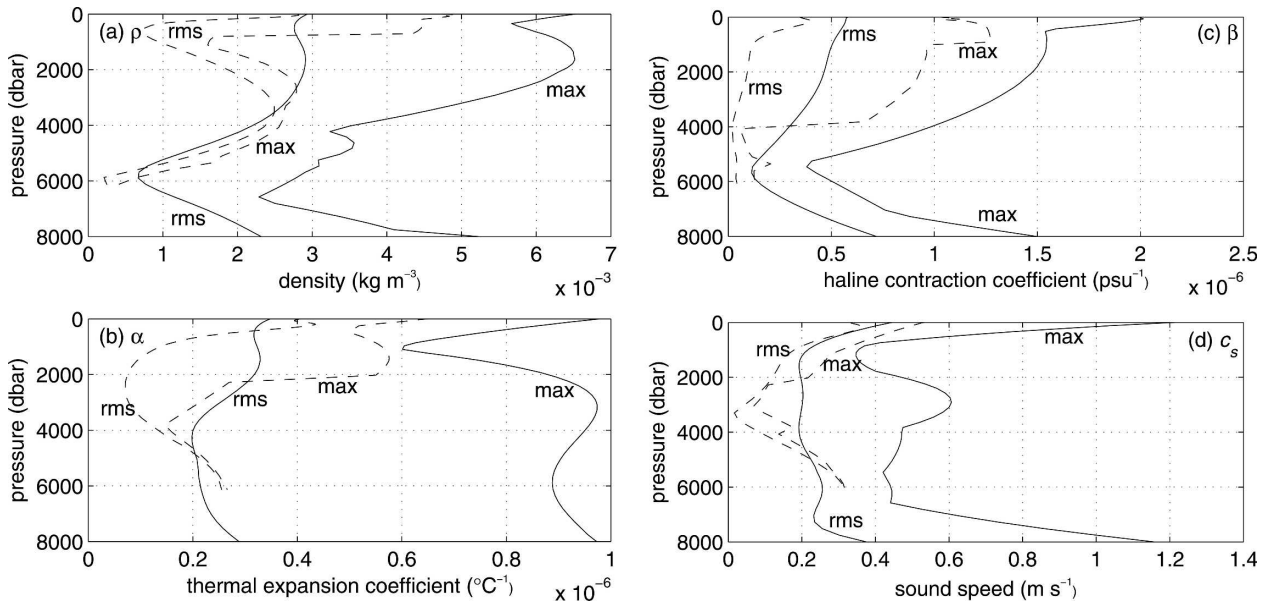


FIG. 2. (a) The rms and the maximum absolute errors in density $\rho(S, \theta, p)$ as a function of pressure for data in the $(S-T-p)$ funnel of Fig. 1 (solid lines). (b)–(d) These error measures for the thermal expansion coefficient, the haline contraction coefficient, and sound speed, respectively. These figures are for the differences between our 25-term equation of state and the full F03 form of the equation of state. Dashed lines are for the climatological data of Koltermann et al. (2004).

those in the thermal expansion coefficient are $2.8 \times 10^{-7} \text{ K}^{-1}$ (rms) and $9.8 \times 10^{-7} \text{ K}^{-1}$ (max), respectively. In terms of real ocean climatology the corresponding errors are $1.9 \times 10^{-3} \text{ kg m}^{-3}$ (rms) and $4.9 \times 10^{-3} \text{ kg m}^{-3}$ (max), and $2.9 \times 10^{-7} \text{ K}^{-1}$ (rms) and $6.5 \times 10^{-7} \text{ K}^{-1}$ (max), respectively. All density and thermal expansion coefficient rms errors of the $\rho(S, \theta, p)$ fit are thus within the uncertainty of both available ocean data and the F03 Gibbs potential fit to this ocean data. For example, the rms error in α in Fig. 2b of $2.8 \times 10^{-7} \text{ K}^{-1}$ is only 38% of the rms error in the α fit of F03 to the underlying data. We therefore have no hesitation using the same rational function here as was used in MJWF03.

On the basis of this comparison of rms errors one concludes that our 25-term equation of state and F03 yield equally accurate estimates of ρ and α . The maximum absolute error in the haline contraction coefficient β in Fig. 2c is approximately $2 \times 10^{-6} (\text{psu})^{-1}$, which corresponds to a relative error of 0.25% of the mean value of β and is thus less important than the corresponding errors in α . The rms errors of the sound speed fit of F03 are at most 3.5 cm s^{-1} when fitting data that has rms errors of 5 cm s^{-1} . This is to be compared with typical rms errors of 26 cm s^{-1} in our equation (Fig. 2d) for both the funnel of data in Fig. 1 and the ocean data of Koltermann et al. (2004). Given that the density computed from the Gibbs potential of F03 contains almost 3 times (73 terms) as many parameters as our 25-term equation of state, there will inevitably be oceanographic variables that F03 will represent more accurately than we can with our density equation. We chose to accurately represent the thermal expansion coefficient with our choice of penalty function and with our choice of terms, and this has been at the expense of the accuracy of sound speed. However, the maximum errors in sound speed in Fig. 2d are still less than the extreme errors of several meters per second that exist between the different sound speed formulas that appear in F03. The comparison of 73 terms for the F03 equation of state to 25 terms for the rational function equation of state also clearly indicates the improved efficiency in using the latter parameterization for ocean density.

3. Algorithms associated with conservative temperature $\Theta(S, \theta)$

The first law of thermodynamics may be written as (Landau and Lifshitz 1959)

$$\rho \left(\frac{dh}{dt} - \frac{1}{\rho} \frac{dp}{dt} \right) = -\nabla \cdot \mathbf{F}_Q + \rho \varepsilon_M,$$

where h is the specific enthalpy, defined by $h \equiv \varepsilon + (p_0 + p)/\rho$, ε is the internal energy, ρ is in situ density, p is the excess of the real pressure over the fixed atmospheric reference pressure, $p_0 = 0.101325 \text{ MPa}$, $d/dt \equiv \partial/\partial t + \mathbf{u} \cdot \nabla$ is the material derivative following the instantaneous fluid velocity, \mathbf{F}_Q is the flux of heat by all manner of molecular fluxes and by radiation, and $\rho \varepsilon_M$ is the rate of dissipation of kinetic energy (in units of W m^{-3}) into thermal energy. The effect of the dissipation of kinetic energy in these equations is very small and is always ignored in the oceanic context. McDougall (2003) has shown that the left-hand side can be approximated by $\rho dh^0/dt$, where h^0 is the potential enthalpy referenced to 0 dbar, with additional terms that are zero at the sea surface and are not larger anywhere than the dissipation of mechanical energy. Hence, the first law of thermodynamics in the ocean can be expressed as $\rho dh^0/dt = -\nabla \cdot \mathbf{F}_Q$. It is this form of the first law that can then be Reynolds averaged to obtain an equation in which the turbulent fluxes of potential enthalpy are much larger than the molecular fluxes of heat so that potential enthalpy is the oceanic variable that encapsulates what we mean by the ‘‘heat content’’ of seawater. That is, potential enthalpy is the variable whose advection and turbulent diffusion throughout the ocean can be accurately compared with the boundary fluxes of heat. The error involved in making this statement is no larger than those associated with ignoring the dissipation of mechanical energy and is two orders of magnitude less than the error that is incurred in the present oceanic practice of treating potential temperature as a conservative variable.

This section of the paper contains three algorithms that are required by an ocean model so that its temperature conservation equation can be an accurate embodiment of the first law of thermodynamics.

a. The forward function $\Theta(S, \theta)$

Conservative temperature is defined to be proportional to potential enthalpy. Full details on the precise definition of conservative temperature Θ as a function of salinity S and potential temperature θ (referred to 0 dbar) can be found in section a of appendix B.

In Fig. 3, we show the differences $\theta - \Theta$ between potential temperature and conservative temperature on the S - Θ diagram. This temperature difference has been deliberately designed to be small for much of the oceanographically relevant regions of S - Θ space. These regions are shaded gray based on real ocean data taken from the Koltermann et al. (2004) climatology. The difference between the present definition of Θ , which is based on the Gibbs function of F03 and that of McDougall (2003) based on the FH95 Gibbs function, is shown

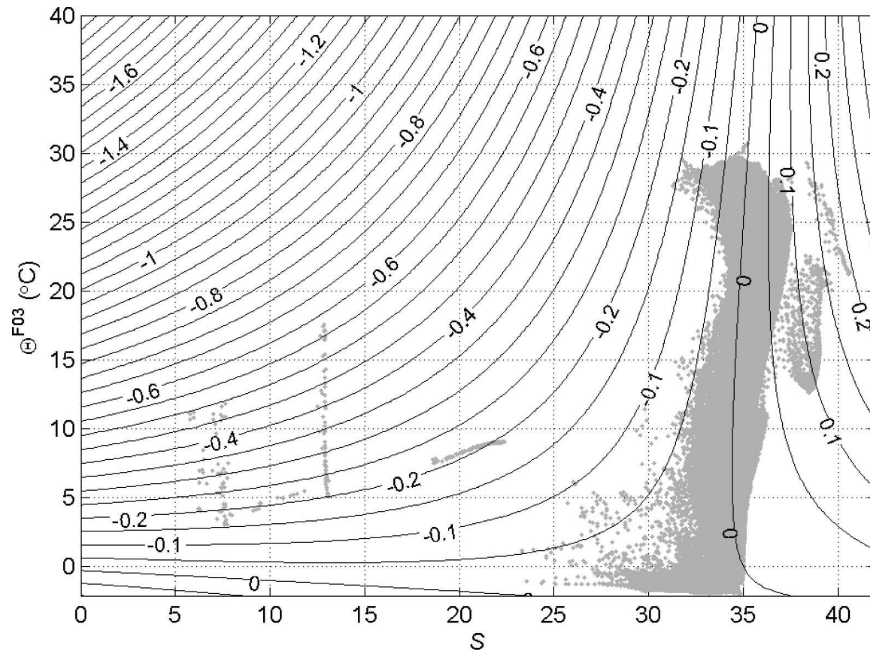


FIG. 3. Differences $\theta - \Theta^{\text{F03}}$ between potential temperature and conservative temperature based on the F03 Gibbs potential over the $S-\Theta^{\text{F03}}$ plane. Also plotted in gray are real ocean data points taken from the Koltermann et al. (2004) climatology.

in Fig. 4. The most obvious feature of Fig. 4 is the linear trend in S , but this is thermodynamically irrelevant because enthalpy is unknown and unknowable up to a linear function of salinity; that is, as explained by FH95,

no thermodynamic measurement can distinguish between two versions of enthalpy that differ by a linear function of salinity. The trend has been caused by shifting the reference point used for pure water from $T =$

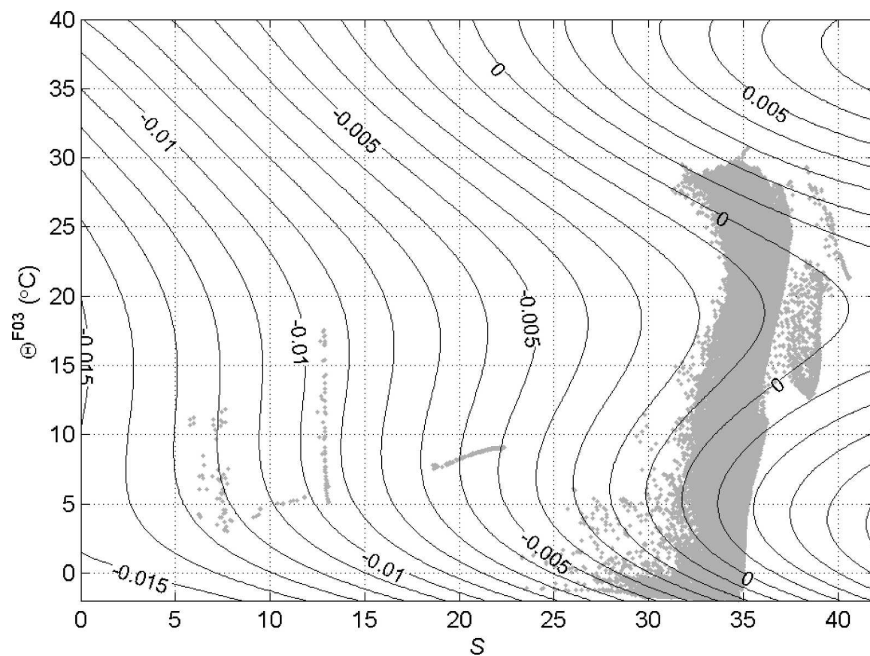


FIG. 4. Differences $\Theta^{\text{FH95}} - \Theta^{\text{F03}}$ between conservative temperature based on the FH95 and the F03 Gibbs potential over the $S-\Theta^{\text{F03}}$ plane. The gray points again correspond to real ocean data points taken from the Koltermann et al. (2004) climatology.

0°C , $p = 0$ dbar in FH95 to the triple point in F03, but with zero offset for the standard ocean, $T = 0^\circ\text{C}$ and $S = 35$ psu. When this linear trend in S is subtracted, one finds that the maximum difference between the two definitions of Θ is only 0.003°C , which is approximately two orders of magnitude less than the differences, $\theta - \Theta$, contained in Fig. 3. This maximum difference of 0.003°C in the two definitions of Θ based on the Gibbs functions of FH95 and F03 is primarily due to the different heat capacity data that was used in those papers to fit the respective Gibbs functions. As explained in F03, the earlier Gibbs function of FH95 [as well as Fofonoff and Millard (1983) heat capacity] was based on quite old heat capacity data of freshwater that were published between 1902 and 1927.

Table 9 of F03 shows that the heat capacity data published in the 1970s, which had an rms error of $0.5 \text{ J (kg K)}^{-1}$, is reproduced by the F03 Gibbs function to an rms accuracy of $0.54 \text{ J (kg K)}^{-1}$. To obtain an estimate of the corresponding error in Θ , we assume that the remaining error in the heat capacity of F03 is of order one-half of this value. Integrating a heat capacity error of $0.25 \text{ J (kg K)}^{-1}$ over a temperature range of 15°C and dividing by a nominal heat capacity, we obtain 0.001°C as an estimate of the rms error in Θ . This is almost the same as the estimate from McDougall (2003) of the accuracy with which Θ is a conservative variable that represents the heat content of seawater. We conclude that the conservative temperature of Eq. (B1) (and Table B1) is more accurate than that based on FH95 and that any remaining uncertainty in Θ is at the level of 1 mK, being approximately equally due to the remaining uncertainty in the Gibbs function of seawater and to the nonconservation of potential enthalpy in the ocean. The practice to date in oceanography essentially has heat content being proportional to θ rather than to Θ , even though we know that the rms and maximum values of $|\theta - \Theta|$ in the World Ocean are 0.018° and 1.4°C , respectively (from McDougall 2003). This does not appear to be justifiable: we recommend adopting the algorithm (B1) and Table B1 as the definition of Θ .

When an ocean model is run with conservative temperature as its temperature variable, the model needs to be initialized with Θ , and one wonders whether it is sufficiently accurate to use an existing ocean atlas that contains the averaged values of S and θ , namely, \bar{S} and $\bar{\theta}$, and simply calculate the initial Θ field as $\Theta(\bar{S}, \bar{\theta})$. This is not quite the same as the averaged value of conservative temperature, $\bar{\Theta}$, because the functional relationship between these variables is nonlinear. Expanding $\Theta(S, \theta)$ as a Taylor series about the mean values \bar{S} and $\bar{\theta}$ and averaging, we find that

$$\bar{\Theta} \approx \Theta(\bar{S}, \bar{\theta}) + \frac{1}{2} \Theta_{\theta\theta} \overline{\theta'^2} + \Theta_{s\theta} \overline{\theta'S'} + \frac{1}{2} \Theta_{ss} \overline{S'^2}$$

where the second-order partial derivatives are evaluated at $(\bar{S}, \bar{\theta})$. As explained after Eq. (B5) of McDougall (2003), the term proportional to $\overline{\theta'S'}$ is larger than the other two so that $\bar{\Theta} - \Theta(\bar{S}, \bar{\theta}) \approx \Theta_{s\theta} \overline{\theta'S'} \approx -1.4 \times 10^{-3} \overline{\theta'S'}$ with S' measured on the practical salinity scale. With perfectly correlated perturbations of magnitude 3°C and 1 psu, the estimated difference $\bar{\Theta} - \Theta(\bar{S}, \bar{\theta}) \approx 4 \text{ mK}$, which is likely small enough to be ignored. These small nonlinear differences in temperature arise because potential temperature is not a conservative variable, so θ should not have been averaged during the process of forming the atlas. The thermodynamic variable that is conserved on mixing at a certain pressure is enthalpy and, when mixing occurs at depth in the ocean, not even Θ is 100% conserved. For example, Eq. (C8) of McDougall (2003) shows that when mixing occurs at a pressure of 600 dbar between water masses that differ in temperature by 2°C , the resulting value of Θ is different from $\bar{\Theta}$ by about 10^{-5}°C . We conclude that the error involved in averaging θ to form a local averaged value is likely to be no more than a few millikelvin, while the error involved with averaging Θ is estimated to be no more than 10^{-5}°C .

b. The $\rho(S, \Theta, p)$ equation of state

With the temperature in an ocean model being regarded as conservative temperature, an equation of state $\rho(S, \Theta, p)$ is needed, that is, an expression for in situ density written in terms of this new temperature variable. The complete details of the form of this equation, its coefficients, and check values can be found in the second subsection of appendix B.

As in section 2b, the funnel used for the evaluation of the rational function is slightly smaller than the funnel used to obtain the fitted rational function. The difference between our 25-term equation of state and the F03 "truth" is illustrated in Fig. 5. Both rms and maximum absolute errors are shown as functions of pressure for data in the $(S-T-p)$ funnel shown in Fig. 1. Also shown are the corresponding rms and extreme errors for the real ocean data of Koltermann et al. (2004). Figure 5a shows that the maximum error in density is less than 0.006 kg m^{-3} , while the rms error is less than half this value. The other panels of Figures 5 show the errors in the thermal expansion coefficient α , the haline contraction coefficient β , and the sound speed c_s , that result from the errors in our 25-term equation of state when compared with the corresponding coefficients obtained

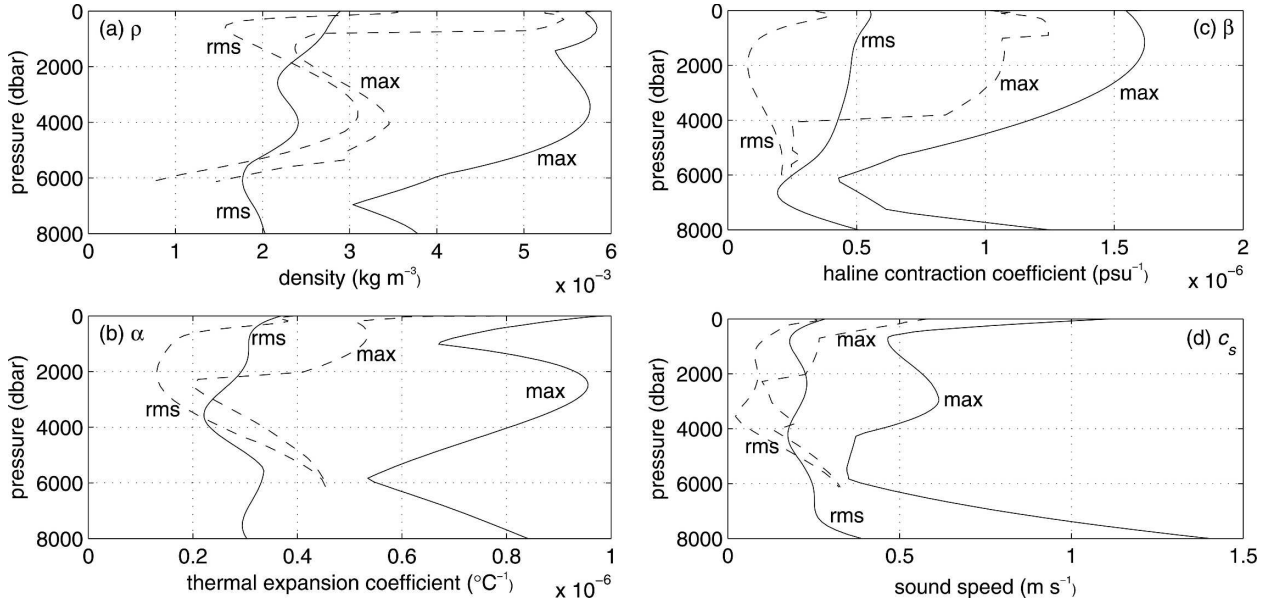


FIG. 5. As in Fig. 2 but for $\rho(S, \Theta, p)$.

using the full Gibbs function of F03. The first derivative coefficients for conservative temperature are defined by

$$\alpha = -\rho^{-1}\partial\rho/\partial\Theta|_{S,p}, \quad \beta = \rho^{-1}\partial\rho/\partial S|_{\Theta,p},$$

$$(c_s)^{-2} = \partial\rho/\partial p|_{S,\Theta}. \quad (1)$$

Note that α and β defined here are slightly different from the corresponding coefficients defined in MJWF03 and section 2b above because in one case differences are taken with respect to (or at constant) Θ and in the other case with respect to (or at constant) θ . In both cases, however, the expressions for the sound speed are the same (since $\partial\rho/\partial p|_{S,\theta} = \partial\rho/\partial p|_{S,\Theta}$) and the buoyancy frequency N can be expressed by the obvious expressions. That is, $g^{-1}N^2 = \alpha\theta_z - \beta S_z$ using the α and β from section 2b, while $g^{-1}N^2 = \alpha\Theta_z - \beta S_z$ when using the α and β from (1). Similarly, the horizontal density gradient is given both by

$$\rho^{-1}\nabla_H\rho - \rho^{-1}(\partial\rho/\partial p)|_{S,\theta}\nabla_H p = \beta\nabla_H S - \alpha\nabla_H\theta,$$

using the α and β from section 2b, and by

$$\rho^{-1}\nabla_H\rho - \rho^{-1}(\partial\rho/\partial p)|_{S,\Theta}\nabla_H p = \beta\nabla_H S - \alpha\nabla_H\Theta,$$

when using the α and β from Eq. (1).

Figure 5b shows that the maximum error in the thermal expansion coefficient is less than $9.9 \times 10^{-7} \text{ }^\circ\text{C}^{-1}$, while the rms value is, apart from the surface mixed layer, less than $3.5 \times 10^{-7} \text{ }^\circ\text{C}^{-1}$. As explained in MJWF03, the key accuracy measure for physical oceanography is this maximum error in the thermal expan-

sion coefficient, which here is equivalent to a relative error in the thermal expansion coefficient of less than 0.7%. The maximum error in the haline contraction coefficient of 1.6×10^{-6} , which corresponds to a relative error of 0.2% of the mean value of β , is thus much less important than the corresponding error in α . As in section 2b, we have not paid much attention to the error in sound speed but we note that the errors in our Fig. 5d are again significantly less than the extreme differences of several meters per second reported in F03 between the various sound speed formulas. In Figs. 5a–d the average values of the rms errors and the maximum absolute errors for the real ocean climatological data of Koltermann et al. (2004) (dashed lines) are consistently less than the corresponding quantities for the larger ocean funnel data. Note, however, that there are substantial pressure intervals over which the rms errors for the ocean climatological data (legitimately) exceed the rms errors for the funnel data of Fig. 1.

The rms error in α of $3.5 \times 10^{-7} \text{ }^\circ\text{C}^{-1}$, shown in Fig. 5b, is only 48% of the rms error in the α derived from the Gibbs function fit of F03 to the underlying data. We have also calculated the differences between the thermal expansion coefficient based on the FH95 Gibbs function and the F03 Gibbs function over the same funnel for both potential and conservative temperature, and find that these differences are about 3 times as large as our maximum error in Fig. 2b and Fig. 5b. This result can also be confirmed from Fig. 21b of F03. We conclude that our 25-term equations of state are as accurate as the data from which F03 was derived and that

there is a marginal increase in accuracy with the update from FH95 to F03.

As in the case of the equation of state in terms of S , θ , and p of section 2b, the equation of state in terms of S , Θ , and p with 25 terms is a substantially more efficient parameterization of ocean density than is the equation of state of F03 with 73 terms. Indeed the rational function equations of state can be coded with only 26 multiplications, one square root, and one division compared with the F03 equation of state that can be coded with 73 multiplications, one square root, and one division, a clear savings in time.

We need to emphasize that the pressure argument in all of these equations of state (including those of FH95, MJWF03, F03, and the present paper) is the gauge pressure in decibars, defined as the absolute pressure in decibars less 10.1325 dbar (see FH95 and F03). The pressure variable in ocean models is sometimes absolute pressure, and the failure to take account of the different definitions of pressure would lead to an error in the thermal expansion coefficient of approximately

$$\delta\alpha = (10.1325\text{db})(\partial\alpha/\partial p)|_{S,\Theta} \approx 2.7 \times 10^{-7} \text{ K}^{-1}$$

[see Fig. 9b of McDougall (1987) for the estimate of $(\partial\alpha/\partial p)|_{S,\Theta}$], which is similar to the rms error in our fit of the thermal expansion coefficient to that of F03. Since this error is virtually constant over the whole ocean, it is clearly more serious than the fitting rms error of this magnitude that is as often positive as negative. Hence, one must be careful to evaluate the equation of state with gauge pressure rather than with absolute pressure.

c. The $\theta(S, \Theta)$ inverse function

During the running of an ocean model the interior temperature is best interpreted as conservative temperature Θ , and the appropriate form of the equation of state is the one expressed in terms of Θ , such as described in section 3b above. If an ocean model is being run with fixed sea surface temperature and fixed sea surface salinity, then the sea surface values of Θ can also be fixed. However, when the ocean is allowed to interact with the atmosphere, the real SST will be needed as an input to the ‘‘bulk formulae’’ for the air–sea heat flux. An inverse algorithm $\theta = \theta(S, \Theta)$ is thus required for converting salinity S and conservative temperature Θ into potential temperature θ . Section c of appendix B contains the full details of this inverse function.

The maximum absolute and rms errors for the computation of potential temperature for 10^4 uniformly generated data points over the $S - \theta$ plane $0 \leq S \leq 42$,

$-2^\circ\text{C} \leq \theta \leq 40^\circ\text{C}$ are, respectively, $6.02 \times 10^{-14} \text{ }^\circ\text{C}$ and $3.78 \times 10^{-15} \text{ }^\circ\text{C}$, justifying the effort in finding a good starting value of θ in (B7) and just one iteration of (B8). These were obtained by first computing conservative temperature using the forward function in section a of appendix B and then inverting using the technology of section c of appendix B. The errors reported above are effectively machine precision, and appear as white noise showing no structure when plotted on the $S - \theta$ plane. As with the algorithm for potential temperature in section 2a, the algorithm for computing potential temperature from conservative temperature here runs 3.5 times as fast as iterating the full Newton–Raphson solution of $\Theta(S, \theta) = \Theta$ to the fixed-point solution with Θ as the initial estimate of potential temperature.

As mentioned above, for an ocean model interacting with the atmosphere, the inverse algorithm for $\theta(S, \Theta)$ will generally need to be used at each model time step to determine the SST at the surface grid level in the ocean. Since this needs to be done only at the one horizontal level and since the computer time involved in evaluating θ is only a couple of times the cost of performing an equation of state evaluation, the computing time required to evaluate SST will not be a significant issue.

4. The freezing temperatures $T_f(S, p)$, $\theta_f(S, p)$, and $\Theta_f(S, p)$

The commonly used algorithm for the calculation of freezing point temperatures is that of Millero and Leung (1976), a four-term polynomial that has been adopted by the United Nations Educational, Scientific and Cultural Organization through Fofonoff and Millard (1983) for the pressure range up to 500 dbar (Millero 1978). The estimated error of this routine when compared to the data of Doherty and Kester (1974) is 3 mK at atmospheric pressure. Its high pressure part is derived by thermodynamic rules (Clausius–Clapeyron equation) and deviates by about the same amount from the data of Fujino et al. (1974) down to a pressure of 500 dbar. Both FH95 and F03 have fitted these same data at one atmosphere, as well as additional more recently available data and standards of freshwater and ice for higher pressures, in F03’s case with an rms error of 1.5 mK. Simplified polynomial expressions for the freezing point based on FH95 were published by Feistel and Hagen (1998). The freezing points given in F03 are computed using a slightly modified version of the former Feistel and Hagen (1998) Gibbs potential of ice, which is to be replaced now by the new and more accurate one of FW05. Here we fit the freezing temperatures of the most recent ice Gibbs function of FW05 to

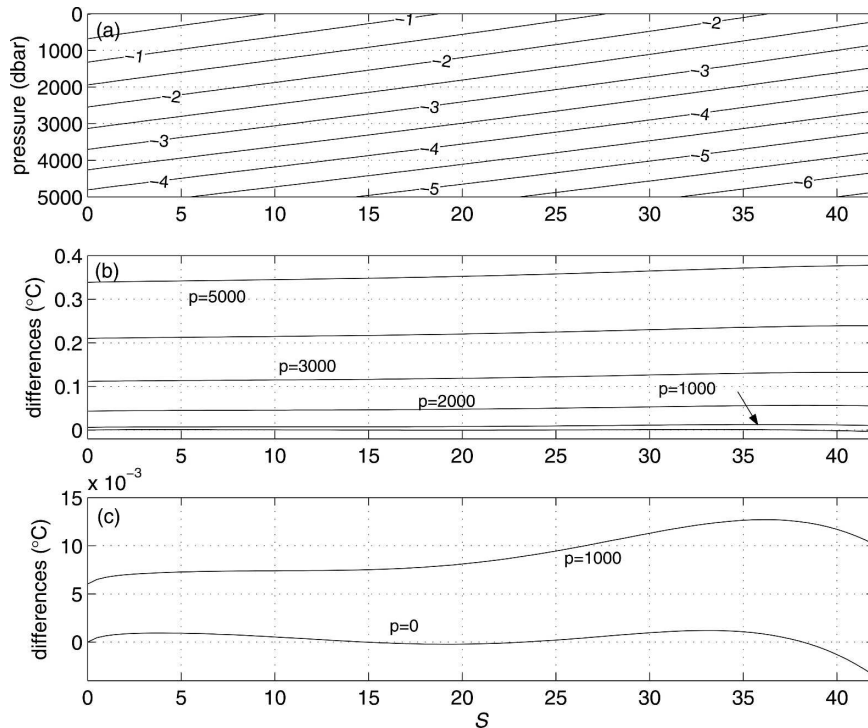


FIG. 6. (a) In situ freezing temperature of seawater and (b), (c) differences between the freezing temperatures of Millero and Leung (1976) and the in situ freezing temperature of seawater, each saturated with air from the solution of (C1)–(C3) and (C5a). Panel (c) is simply an expanded view of (b).

within the same error tolerances as the F03 fit to data, using 11-term rational functions (with only nine unknown parameters). Three fits are made, one for each of the temperature variables—in situ temperature T , potential temperature θ , and conservative temperature Θ . Complete details can be found in appendix C.

Figure 6a shows the (in situ) freezing temperature of air-saturated seawater as a function of salinity and pressure, showing the strong linear dependence on both salinity and pressure. The differences between the formula of Millero and Leung (1976) and the freezing temperatures from the full Newton–Raphson iterative solution to (C1)–(C3) [and using (C5)] are displayed in Figs. 6b and 6c. It is seen that at a pressure of 1000 dbar the error in the Millero and Leung (1976) formula is about 12.5 mK near $S = 35$ psu. The error increases at higher pressures so that at 3000 dbar the error is 130 mK. Corresponding residuals, again relative to the solution of (C1)–(C3) using (C5), for the three freezing temperatures defined by (C5) and (C4) are shown in Fig. 7. All residual plots are for saturated freezing temperatures and are plotted as functions of salinity for a range of pressures. Figure 7 clearly shows that the maximum errors in our fit at $p = 2000$ dbar are of order 1 mK for each of the three temperature variables,

whereas the error in the Millero and Leung (1976) polynomial is of order 50 mK at this pressure.

Even in cases of negative lapse rates, that is, when a water parcel cools down by compression (McDougall and Feistel 2003), the freezing point lowering by pressure (Clausius–Clapeyron equation) significantly exceeds the adiabatic cooling (Feistel and Wagner 2005). Thus, independent of the salinity of a given liquid water parcel, freezing due to pressure change can only occur during expansion (rising) and never during compression (sinking). In other words, freezing of a parcel is impossible at any depth as long as its potential temperature is higher than its surface (in situ) freezing point.

The FW05 freezing point for pure air-free water at one atmosphere is accurate with only 2 μ K error, and it reproduces the Doherty and Kester (1974) freezing points of seawater at atmospheric pressure within their experimental scatter of 2 mK. Due to the significantly more accurate compressibility of ice in the FW05 formulation in comparison to various values discussed in the literature (Dorsey 1968; Yen 1981) and the ones used by Millero (1978) or in FH95 and F03, the high-pressure freezing point measurements of Henderson and Speedy (1987) for pure water are met now within

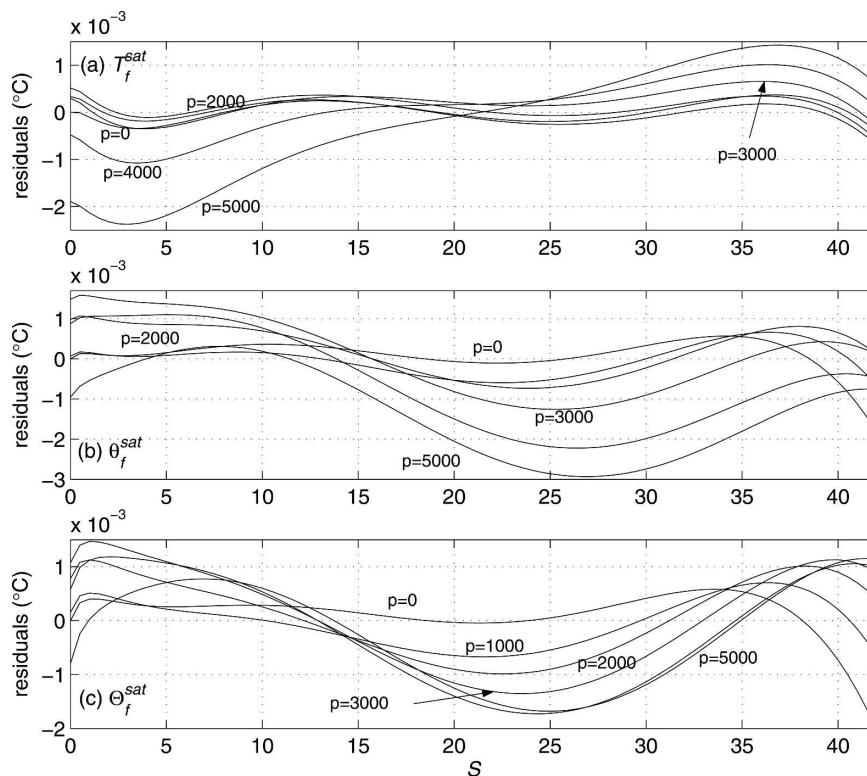


FIG. 7. Residuals between the air saturated freezing temperatures of seawater from Eqs. (C4) and (C5) for (a) in situ temperature, (b) potential temperature, and (c) conservative temperature and saturated freezing temperatures based on the solution of (C1)–(C3). Note the differences in vertical scales between this figure and the residuals in Figs. 6b and 6c.

30 mK up to 10 000 dbar. A similar accuracy can be assumed for the current formula of the freezing temperature of seawater under pressure, even if the extrapolation error of the Gibbs function of seawater down to about -11°C is difficult to quantify. Since the error of present practice is about 300 mK at 5000 dbar (see Fig. 6b), the current freezing point formula offers at least a factor of 10 improvement in the freezing temperature at higher pressures. See FW05 for a more detailed discussion of different freezing point formulas of water and seawater.

5. Salinity versus salt concentration

Practical salinity S of a seawater sample is defined in terms of the sample's electrical conductivity, its temperature, and its pressure (Fofonoff and Millard 1983). The definition involves two separate parts, the first being a reference value that defines the conductivity of a seawater sample with $S = 35$ psu, $T = 15^{\circ}\text{C}$, and $p = 0$ dbar and the second part being an algorithm for the conductivity ratio as a function of salinity, temperature, and pressure. The reference part of the definition as-

signs a salinity of 35 psu to a seawater sample if at 15°C (on the temperature scale IPTS-68) and at zero gauge pressure it has the same conductivity as a potassium chloride solution with a KCl concentration of 32.4356 g kg^{-1} at that temperature and pressure. The second part of the definition (the conductivity ratio) was found by known dilution and evaporation of a single batch of seawater (see Fofonoff 1985). This process of dilution and concentration was designed to make salinity a conservative variable. Note that practical salinity, being defined only in terms of the conductivity, temperature, and pressure of seawater, is not directly related to the chlorinity of seawater nor to the absolute salinity S_A , which is defined as (1000 times) the mass of dissolved substances per mass of solution. While practical salinity does not have any dimensions or units, it is often loosely quoted in practical salinity units, for example, as 35 psu, simply to indicate that the salinity has been determined using the practical salinity scale.

If every parcel of seawater had the same ratio of dissolved substances as the original batch of standard seawater that was used to deduce the algorithm for conductivity ratio, then, indeed, practical salinity would

be a conservative variable (i.e., S would be exactly proportional to the conservative variable S_A), at least to the accuracy with which the conductivity ratio measurements were made and the algorithm was fitted to that data. Even in the major ocean basins there are small variations of the ratio of dissolved substances in seawater that affect density, conductivity, and absolute salinity in ways that are not taken into account by the definition of practical salinity or by the Gibbs function of seawater of F03. There are two related issues here; the first is the relationship of the measured conductivity (and therefore, by definition, practical salinity S) to absolute salinity, and the second is the connection to density. The first issue is the subject of this section of the paper.

To relate practical salinity S to absolute salinity S_A one needs to know the concentrations of all the constituents of seawater, and Millero and Leung (1976) estimated the relationship [where S_A is in parts per thousand [ppt (or ‰)]] as

$$S_A = 1.004\,880\,S. \quad (2a)$$

This relationship was updated by F03 using Millero's (1982) mass fractions of seawater constituents to

$$S_A = 1.004\,867\,S. \quad (2b)$$

[Note that we have corrected an obvious typographical error in Eq. (53) of F03; Feistel 2004.] However, the calculation is sensitive to the ratio of ingredients that are taken to compose seawater, and taking the list of constituents from Culkin (1965) leads to the alternative linear relationship (Fofonoff 1992)

$$S_A = 1.0040\,S. \quad (2c)$$

It is clearly not straightforward to relate absolute salinity S_A to practical salinity S . Nevertheless, setting aside marginal seas, we take as a working hypothesis that in the major ocean basins S_A lies in the range given by Eqs. (2a)–(2c); namely,

$$S_A = (1.0045 \pm 0.0005)\,S. \quad (2d)$$

Note that the freshwater concentration (FW) in seawater is given by

$$\text{FW} = (1 - 0.001S_A) \approx (1 - 1.0045 \times 10^{-3}\,S). \quad (3)$$

The approximately $0.45 \pm 0.05\%$ difference between S and S_A is not trivial; for example, a seawater parcel with $S = 35$ psu has an absolute salinity S_A of between 35.140 and 35.175 ppt, a difference of approximately

0.16 ppt, which is between 50 and 100 times as large as the accuracy with which we can determine salinity at sea. Ocean models interact with the atmosphere (through the evaporation and precipitation $E - P$ of freshwater) as though the variable that is labeled salinity in the model is actually absolute salt concentration S_A (in ppt), and yet in other parts of ocean model code the salinity is regarded as practical salinity (for example in the equation of state). We ask here what is the correct interpretation of the model's salinity and also whether ocean models suffer any significant error due to the different definitions of salinity.

Interpreting the model's salinity as absolute salinity S_A , evaporation and precipitation cause the tendency of absolute salinity $(S_A)_t$ of the uppermost model box to be proportional to the product $S_A (E - P)$. With the interpretation of the model's salinity as practical salinity S , the salinity tendency of the uppermost model layer includes a contribution $S_t \propto S (E - P)$ associated with the surface freshwater fluxes. Given our present knowledge of seawater thermodynamics, it seems reasonable to assume that S is exactly proportional to S_A , and in this case there is actually no error involved with the present implementation of the surface freshwater boundary condition if the model salinity is interpreted as S . That is, existing ocean models have $E - P$ affecting S in exactly the correct manner, just as $E - P$ would affect S_A if the model variable were interpreted as S_A . The combination of (i) the lack of any separate flux of salt across the sea surface and (ii) the exact proportionality of S and S_A enables the present surface boundary condition to be exact. [As a counterexample, if there happened to be a surface input of buckets of crystalline sea salt (in units of kilograms of salt per square meter), then this would be accurately accounted for in the S_A budget but not in the budget of practical salinity S .] As far as the rest of the model domain is concerned, the salt conservation equation is equally true whether written in terms of S_A or in terms of S , and with the equation of state in today's models being expressed as a function of S , models are calculating density consistently.

In summary, it seems that, despite the fact that practical salinity is not the same as absolute salinity, present models do not incur errors when they relax their salinity to values of S when they interact with an atmosphere through freshwater fluxes, when they advect and diffuse S , and when they evaluate the equation of state in terms of practical salinity. Hence, it would seem that the interpretation of the model variable as practical salinity S is error free. The only slight complication is that, when one wants to calculate the freshwater frac-

tion exactly, one needs to use the expression from (3), namely, $FW \approx (1 - 1.0045 \times 10^{-3} S)$ and, strictly speaking, this should be used when calculating the meridional flux of freshwater for an ocean basin (e.g., the Indian Ocean or the South Pacific Ocean). Also, modern ice models allow for ice that is not completely fresh but rather contains small amounts of salt, and this slightly salty ice is exchanged with the ocean as water freezes and melts. It is assumed that the salinity of this ice can be interpreted as being measured on the practical salinity scale rather than as absolute salinity, and in this case, no error would be incurred in the interaction between ice and ocean.

An alternative modeling approach is to interpret the model's salinity as absolute salinity. To be able to interpret the model's salinity as S_A , three changes to present modeling practice are required: first in the restoring boundary condition (if used) where the restoration would need to be to fixed values of S_A rather than of S , second in the equation of state which would need to be written in the functional form $\rho(S_A, \Theta, p)$ rather than as $\rho(S, \Theta, p)$, and third in the initial conditions for a model run where it is imperative that the initial salinity field is S_A rather than S . If this third point were not done, the total amount of salt in the ocean would be in error by 0.45% for the whole model run, as there is no salt flux into or out of the ocean unless a restoring boundary condition is employed. With these three changes, the freshwater content and freshwater fluxes could then be evaluated exactly using $FW = (1 - 0.001 S_A)$, and the salinity of sea ice would also be interpreted as being absolute salinity. These three changes to modeling practice could readily be implemented if it was deemed important to be able to determine the freshwater content directly in terms of the model's salinity variable but, at this point, it is not obvious that this is a significant issue.

6. Discussion

One of the aims of the present work is to update the algorithms of McDougall et al. (2003) for the computation of potential temperature and density of seawater. The new algorithms are based on the latest seawater Gibbs potential of Feistel (2003), which is an improvement over the earlier Gibbs potential of Feistel and Hagen (1995) in both computational accuracy and in the extent of the oceanic data utilized in the formulation of the Gibbs potential. We have also determined a function for computing the freezing temperature of seawater that is consistent with the latest Gibbs potentials

of seawater (Feistel 2003) and ice (Feistel and Wagner 2005).

Various algorithms involving the new conservative temperature variable of McDougall (2003) have also been presented. These include the definition of conservative temperature from the potential enthalpy function of Feistel (2003), together with a function for the density of seawater written in terms of conservative temperature and an inverse function for computing potential temperature from salinity and conservative temperature. All conservative temperature routines are based on the Feistel (2003) Gibbs potential.

Although the rms and maximum absolute differences relative to F03 for the two density equations reported here are larger than the corresponding differences relative to FH95 for the density equation of McDougall et al. (2003), the rms differences for density and the thermal expansion coefficient are still below the corresponding rms errors present in both the Feistel (2003) fits and in the oceanic data underlying these fits. Following MJWF03, we have concentrated on the relative errors in the thermal expansion coefficient and in the saline contraction coefficient, as these are the only errors in the equation of state that have dynamical consequences in ocean models. As explained in MJWF03, any error in density that is a function only of pressure and is independent of salinity and conservative temperature does not affect ocean dynamics either through the computation of horizontal pressure gradients or in the calculation of vertical static stability.

From Figs. 5a and 5b of MJWF03 we see that the maximum errors in density and thermal expansion of the International Equation of State over the volume of our funnel are $\pm 0.012 \text{ kg m}^{-3}$ and $\pm 2.5 \times 10^{-6} \text{ K}^{-1}$, while the present Figs. 2 and 5 show that the corresponding maximum errors are about $\pm 0.006 \text{ kg m}^{-3}$ and $\pm 0.95 \times 10^{-6} \text{ K}^{-1}$. These measures of accuracy are only relevant if the F03 Gibbs function is equally as accurate. This question can be addressed by the comparison of F03 densities with the measurements of Bradshaw and Schleicher (1970) and also by considering how well the F03 Gibbs function reproduces the measurements of the temperature of maximum density (TMD). Bradshaw and Schleicher measured differences in specific volume as temperature varied at fixed pressure and salinity for samples in the salinity range between 30 and 40 psu. Figure 24a of F03 shows that the Bradshaw and Schleicher (1970) data is fitted by the F03 Gibbs function with a maximum density error of no more than $\pm 0.004 \text{ kg m}^{-3}$ in the range of temperatures and pressures in our funnel. This amounts to an upper bound on the thermal expansion coefficient of F03 for

oceanographic data from our funnel of no more than $\pm 0.4 \times 10^{-6} \text{ K}^{-1}$ in the salinity range $30 < S < 40$ psu.

Measurements of the TMD data of Caldwell (1978) provide a rather direct estimate of the accuracy of the thermal expansion coefficient for very cold and fresh seawater. From Table 9 of F03, we see that the rms error in the thermal expansion coefficient derived from F03 is $\pm 0.73 \times 10^{-6} \text{ K}^{-1}$ with respect to the TMD data of Caldwell (1978). This fitting error is also approximately the experimental error in the TMD data itself.

Taking this and the agreement between F03 and the Bradshaw and Schleicher (1970) specific volume data means that it is very likely that the maximum density error in the range of temperatures and pressures in our funnel in Figs. 2 and 5 is no more than $\pm 0.006 \text{ kg m}^{-3}$, while the maximum error in our thermal expansion coefficients is $\pm 0.95 \times 10^{-6} \text{ K}^{-1}$. In the salinity range $30 < S < 40$ psu, typical of values in the ocean atlas, it seems that the absolute accuracy of our algorithms for density and thermal expansion for water of standard composition may be $\pm 0.005 \text{ kg m}^{-3}$ and $\pm 0.6 \times 10^{-6} \text{ K}^{-1}$, respectively.

Another uncertainty remaining in the equation of state and in the determination of salinity from oceanic observations is due to spatial variations in the relative concentrations of alkalinity, total carbon dioxide, and silica. Brewer and Bradshaw (1975) and, more recently, Millero (2000) have shown that for given values of conductivity, temperature, and pressure the range of uncertainty of density is up to 0.020 kg m^{-3} between the major ocean basins; we will characterize this uncertainty as $\pm 0.010 \text{ kg m}^{-3}$. Since the maximum density error of the International Equation of State (Fofonoff and Millard 1983) is about $\pm 0.012 \text{ kg m}^{-3}$ and the maximum error in the present equation of state is $\pm 0.005 \text{ kg m}^{-3}$, we conclude that the uncertainty in oceanic composition is as serious as the errors in the International Equation of State of standard seawater and is a larger issue (by a factor of 2) than any remaining uncertainty in either F03 or the fit to F03 contained in the present work. One could imagine mounting a concerted campaign to reduce these errors by, for example, obtaining more accurate measurements of the temperature of maximum density so as to improve the accuracy of the thermal expansion coefficient. However, this activity would only be worthwhile if one could simultaneously address the issues raised by Millero (2000) to account for the variation of the composition of seawater.

The rms errors in our freezing temperature equation are of the same order as the rms errors in the freezing temperatures in F03, and the present freezing temperature equations are much more accurate than the equation in use today.

Oceanography traditionally uses salinity evaluated on the practical salinity scale S , but the freshwater concentration of seawater is not $(1 - 0.001 S)$ but, rather, is given in terms of the absolute salt concentration S_A by $(1 - 0.001 S_A)$. Even though S and S_A differ by about 0.45%, because the air–sea interaction involves only fluxes of freshwater and not of salt, we have shown that ignoring the distinction between S and S_A does not cause errors of this magnitude.

Of the remaining issues with the equation of state and the thermodynamics of seawater, the largest that needs to be addressed by ocean models is the changing of an ocean model's temperature variable from potential temperature θ to conservative temperature Θ since a typical maximum error in $\theta - \Theta$ of 0.25°C causes a density difference of 0.05 kg m^{-3} . This is a factor of at least 5 larger than the density errors that we believe remain due to the uncertainty in the equation of state. (Actually, $\theta - \Theta$ is as large as 1.4°C in restricted areas of the World Ocean.)

Another temperature-like variable can be defined as proportional to specific entropy [see Fig. 5 of McDougall (2003)], but from the second law of thermodynamics, we know that entropy is not a conservative variable since there is a net production of entropy whenever diffusion and mixing occur. Hence, it is clearly not appropriate as an approximation to "heat content" in the ocean. However, one finds that the rms and maximum absolute differences between this "entropic temperature" and Θ are 0.33° and 0.5°C , respectively, so for extreme water masses (particularly for warm freshwater) entropy is actually closer to being a conservative variable than is potential temperature. An alternative measure of the errors associated with these variables is the range of temperature differences outside of which 1% of the data reside. McDougall (2003) reports that 1% of the $\theta - \Theta$ values at the sea surface of the World Ocean lie outside an error range of 0.25°C ($-0.15^\circ\text{C} < \theta - \Theta < 0.10^\circ\text{C}$), which provides a convenient measure of the error associated with ocean models that treat θ as conservative. The corresponding analysis for entropic temperature shows that 1% of the surface data lie outside an error range of 0.53°C (0.5% have a temperature difference less than -0.21°C and 0.5% exceed a difference of 0.32°C). This error measure suggests that θ is only about a factor of 2 more conservative than entropy. It seems clear that θ is also not an appropriate approximation to the conservative heat content of seawater. It is probably time to abandon this practice.

Software for the algorithms described in this paper can be obtained on the Internet (available online at www.marine.csiro.au/~jackett/eos).

TABLE A1. Coefficients of the seven-term approximating polynomial θ_0 for potential temperature [see Eqs. (A3) and (A4) of MJWF03].

a_1	8.654 839 133 954 42 $\times 10^{-6}$	a_5	2.839 333 685 855 34 $\times 10^{-8}$
a_2	-1.416 362 997 448 81 $\times 10^{-6}$	a_6	1.778 039 652 186 56 $\times 10^{-8}$
a_3	-7.382 864 671 357 37 $\times 10^{-9}$	a_7	1.711 556 192 082 33 $\times 10^{-10}$
a_4	-8.382 413 570 396 98 $\times 10^{-6}$		

Acknowledgments. This work is a contribution to the CSIRO Climate Change Research Program.

APPENDIX A

Algorithms Based on Potential Temperature

a. Updated coefficients for potential temperature $\theta(S, T, p, p_r)$

The potential temperature of a fluid parcel (S, T, p) when referenced to a pressure p_r is defined as that temperature θ for which

$$\sigma(S, \theta, p_r) = \sigma(S, T, p), \quad (\text{A1})$$

where specific entropy σ is given by the first derivative of the Gibbs potential $g(S, T, p)$ with respect to temperature, $\sigma(S, T, p) = -\partial g(S, T, p)/\partial T$. The solution of (A1) is achieved with the modified Newton–Raphson technique described in MJWF03. The only coefficients requiring updating from MJWF03 are the coefficients for the initial rational function approximation for θ and the constant first guess for σ_T at constant S and $p = p_r$. Otherwise, all details are exactly as in MJWF03. Table A1 contains the new rational function coefficients while $13.6 \text{ J kg}^{-1} \text{ K}^{-1}$ is the (constant) first estimate of σ_T . We recommend two iterations of this technique that yield rms and maximum absolute errors of $3.50 \times 10^{-15} \text{ }^\circ\text{C}$ and $2.84 \times 10^{-14} \text{ }^\circ\text{C}$, respectively, when compared to the fixed-point Newton–Raphson solutions of (A1). A check value for the new potential temperature algorithm is

$$\theta(35, 20, 4000, 0) = 19.2110837430117^\circ\text{C}.$$

Note that this calculation of potential temperature reproduces the potential temperatures of Table 19 of F03.

b. Updated coefficients for the density equation $\rho(S, \theta, p)$

The 25-term equation of state for in situ density (in kg m^{-3}), when expressed as a function of salinity S (PSS-78), potential temperature θ (in $^\circ\text{C}$), and pressure p (in dbar), is taken to have the same form as the corresponding equation in MJWF03; namely,

$$\rho(S, \theta, p) = P_n(S, \theta, p)/P_d(S, \theta, p), \quad (\text{A2})$$

where the polynomials $P_n(S, \theta, p)$ and $P_d(S, \theta, p)$ are defined as in Table A2. Here θ is potential temperature referenced to $p_r = 0$. Values for these coefficients were found by fitting 2×10^4 uniformly distributed points in (S, T, p) space to in situ density values obtained by differentiating the Gibbs potential of F03 with respect to pressure and using

$$1/\rho(S, T, p) = \partial g(S, T, p)/\partial p.$$

These points were taken from the larger funnel that is described in section 2b. The corresponding potential temperature values were computed by iterating the standard Newton–Raphson solution for solving (A1) to the fixed (potential temperature) points.

A check value for this density equation is $\rho(35, 25, 2000) = 1031.650\,560\,565\,76 \text{ kg m}^{-3}$, corresponding to $S = 35 \text{ psu}$, $\theta = 25^\circ\text{C}$, and $p = 2000 \text{ dbar}$. Other check values are $\rho(20, 20, 1000) = 1017.728\,868\,019\,64 \text{ kg m}^{-3}$ and $\rho(40, 12, 8000) = 1062.952\,798\,206\,31 \text{ kg m}^{-3}$. Over the very large $(S-\theta-p)$ cube $[0, 50 \text{ psu}] \times [-10^\circ\text{C}, 50^\circ\text{C}] \times [0 \text{ dbar}, 10^4 \text{ dbar}]$, $P_n(S, \theta, p)$ and $P_d(S, \theta, p)$ are very well behaved; $P_n(S, \theta, p)$ varies smoothly from 920 to almost 1500, while $P_d(S, \theta, p)$ varies smoothly from 0.92 to about 1.4. Finally, the evaluation of potential density relative to reference pressure p_r is simply $\rho(S, \theta, p_r)$ for a water parcel with salinity S and potential temperature θ (referenced to 0 dbar); there is no need to calculate potential temperature referenced to p_r in order to calculate potential density referenced to p_r .

APPENDIX B

Algorithms Based on Conservative Temperature

a. The forward function $\Theta(S, \theta)$

The definition of Θ , based on potential enthalpy $h^0(S, \theta) = h(S, \theta, 0)$, is

$$\Theta = \Theta(S, \theta) \equiv h^0(S, \theta)/C_p^0, \quad (\text{B1})$$

where $C_p^0 \equiv h(S = 35, \theta = 25, p = 0)/(25^\circ\text{C}) = 3992.103\,223\,296\,49 \text{ J kg}^{-1} \text{ K}^{-1}$. It follows that $\Theta(S = 35, \theta = 25) = 25^\circ\text{C}$. Enthalpy $h(S, T, p)$ is computed from the Gibbs potential $g(S, T, p)$, according to $h(S, T, p) = g(S, T, p) - (T + 273.15 \text{ }^\circ\text{C}) \partial g(S, T, p)/\partial T$. Being a so-called thermochemical property of seawater, enthalpy cannot be obtained from the current standard formula of Fofonoff and Millard (1983). As in F03, the power series for potential enthalpy $h^0(S, \theta)$ is written in

TABLE A2. Terms and coefficients of the polynomials $P_n(S, \theta, p)$ and $P_d(S, \theta, p)$ that define the rational function equation of state [Eq. (A2)].

$P_n(S, \theta, p)$	Coefficients	$P_d(S, \theta, p)$	Coefficients
Constant	$9.998\,408\,544\,484\,934\,7 \times 10^2$	Constant	1.0
θ	$7.347\,162\,586\,098\,158\,4 \times 10^0$	θ	$7.281\,521\,011\,332\,709\,1 \times 10^{-3}$
θ^2	$-5.321\,123\,179\,284\,176\,9 \times 10^{-2}$	θ^2	$-4.478\,726\,546\,198\,392\,1 \times 10^{-5}$
θ^3	$3.649\,243\,910\,981\,454\,9 \times 10^{-4}$	θ^3	$3.385\,100\,296\,580\,243\,0 \times 10^{-7}$
S	$2.588\,057\,102\,399\,139\,0 \times 10^{+0}$	θ^4	$1.365\,120\,238\,975\,857\,2 \times 10^{-10}$
$S\theta$	$-6.716\,828\,278\,669\,235\,5 \times 10^{-3}$	S	$1.763\,212\,666\,904\,037\,7 \times 10^{-3}$
S^2	$1.920\,320\,205\,5760151 \times 10^{-3}$	$S\theta$	$-8.806\,658\,325\,120\,647\,4 \times 10^{-6}$
p	$1.179\,826\,374\,043\,036\,4 \times 10^{-2}$	$S\theta^3$	$-1.883\,268\,943\,480\,489\,7 \times 10^{-10}$
$p\theta^2$	$9.892\,021\,926\,639\,911\,7 \times 10^{-8}$	$S^{3/2}$	$5.746\,377\,674\,543\,209\,7 \times 10^{-6}$
pS	$4.699\,664\,277\,175\,473\,0 \times 10^{-6}$	$S^{3/2}\theta^2$	$1.471\,627\,547\,224\,233\,4 \times 10^{-9}$
p^2	$-2.586\,218\,707\,515\,435\,2 \times 10^{-8}$	p	$6.710\,324\,628\,565\,189\,4 \times 10^{-6}$
$p^2\theta^2$	$-3.292\,141\,400\,796\,066\,2 \times 10^{-12}$	$p^2\theta^3$	$-2.446\,169\,800\,702\,458\,2 \times 10^{-17}$
		$p^3\theta$	$-9.153\,441\,760\,428\,906\,2 \times 10^{-18}$

terms of the scaled salinity and potential temperature variables $s = S/40$ and $\tau = \theta/40^\circ\text{C}$. The coefficients of the polynomial $h^0(s, \tau)$ are contained in Table B1, and check values for conservative temperature are $\Theta(20 \text{ psu}, 20^\circ\text{C}) = 20.452\,749\,612\,827\,6^\circ\text{C}$, $\Theta(0 \text{ psu}, 0^\circ\text{C}) = 0.015\,283\,578\,793\,549\,1^\circ\text{C}$, $\Theta(35 \text{ psu}, 0^\circ\text{C}) = 0^\circ\text{C}$, and $\Theta(35 \text{ psu}, 25^\circ\text{C}) = 25^\circ\text{C}$.

As explained in the appendix of McDougall and Feistel (2003), once one knows entropy as a function of salinity and conservative temperature, specific enthalpy expressed as a function of S , Θ , and p can be used as a thermodynamic potential from which all quantities of thermodynamic interest can be derived. This functional form $h(S, \Theta, p)$ is the sum of potential enthalpy and a pressure integral of the specific volume; namely,

$$h(S, \Theta, p) = h^0 + \int_0^p \frac{1}{\rho(S, \Theta, p')} dp' \\ = C_p^0 \Theta + \int_0^p \frac{1}{\rho(S, \Theta, p')} dp'. \quad (\text{B2})$$

The form of the rational function for density, (B5), of the next section is specifically chosen so that it can be integrated analytically with respect to pressure [see section 2.103 of Gradshteyn and Ryzhik (1980)]. The rather compact formulas for density ρ , adiabatic compressibility κ , sound speed c , and the adiabatic lapse rate Γ , are then

$$\rho^{-1} = h_p; \kappa = -h_{pp}/h_p; c^{-2} = -h_{pp}/(h_p)^2; \Gamma = h_{p\Theta}/\sigma_\Theta. \quad (\text{B3})$$

Also following McDougall and Feistel (2003), potential temperature θ and the absolute in situ temperature T can be found in terms of Θ from

$$(T_0 + \theta) = C_p^0/\sigma_\Theta; \\ (T_0 + T)/(T_0 + \theta) = h_\Theta(S, \Theta, p)/C_p^0 \\ = \partial h/\partial h^0|_{S,p}, \quad (\text{B4})$$

where $T_0 = 273.15^\circ\text{C}$. Since the thermodynamic quantities of primary interest in physical oceanography can be evaluated directly from density, we do not further pursue the consequences of treating $h(S, \Theta, p)$ as the thermodynamic potential function.

b. The $\rho(S, \Theta, p)$ equation of state

The form adopted for the equation of state in terms of salinity S , conservative temperature Θ , and pressure p is identical to the form of the equation of state in terms of S , potential temperature θ , and pressure p of MJWF03 and section 2b above. That is, we use a rational function with a 12-term polynomial in the numerator and a 13-term polynomial in the denominator. The procedure for fitting the equation of state with Θ is precisely the same as the procedure used for fitting the $\rho(S, \theta, p)$ equation of state, and we have used the same funnel of oceanic data as before. For each data point in the funnel in (S, T, p) space we first find potential temperature θ referenced to $p_r = 0$, and in situ density $\rho(S, T, p)$ from the accurate expression found by differentiating the F03 Gibbs function with respect to pressure. Conservative temperature Θ is then found from Eq. (B1) of the previous section.

The 25-term equation of state can be written as

$$\rho(S, \Theta, p) = \frac{P_n(S, \Theta, p)}{P_d(S, \Theta, p)} \quad (\text{B5})$$

where $P_n(S, \Theta, p)$ and $P_d(S, \Theta, p)$ are polynomials defined as in Table B2. A check value for this equation is $\rho = 1031.652\,123\,323\,55 \text{ kg m}^{-3}$, corresponding to $S = 35 \text{ psu}$, $\Theta = 25^\circ\text{C}$ (where $\theta = 25^\circ\text{C}$ also), and $p = 2000$

TABLE B1. Terms and coefficients of the polynomial for potential enthalpy $h^0(s, \tau)$ for the scaled salinity and potential temperature variables $s = S/40$ and $\tau = \theta/40^\circ\text{C}$.

$h^0(s, \tau)$ terms	Coefficients	$h^0(s, \tau)$ terms	Coefficients
Constant	$6.101\ 362\ 416\ 523\ 295\ 5 \times 10^1$		
τ	$1.687\ 764\ 613\ 804\ 801\ 5 \times 10^5$	$s\ \tau^4$	$3.039\ 107\ 198\ 280\ 803\ 5 \times 10^2$
τ^2	$-2.735\ 278\ 560\ 511\ 964\ 3 \times 10^3$	$s\ \tau^5$	$6.974\ 975\ 368\ 852 \times 10^1$
τ^3	$2.574\ 216\ 445\ 382\ 144\ 2 \times 10^3$	$s^{1.5}$	$9.379\ 793\ 807\ 560\ 891 \times 10^2$
τ^4	$-1.536\ 664\ 443\ 497\ 754\ 5 \times 10^3$	$s^{1.5}\ \tau$	$2.167\ 720\ 825\ 960\ 16 \times 10^3$
τ^5	$5.457\ 340\ 497\ 931\ 63 \times 10^2$	$s^{1.5}\ \tau^2$	$-1.224\ 577\ 280\ 056\ 290\ 2 \times 10^3$
τ^6	$-5.091\ 091\ 728\ 474\ 333\ 4 \times 10^1$	$s^{1.5}\ \tau^3$	$3.263\ 074\ 029\ 273\ 967 \times 10^2$
τ^7	$-1.830\ 489\ 878\ 927\ 802 \times 10^1$	$s^{1.5}\ \tau^4$	$5.067\ 038\ 246\ 895\ 18 \times 10^1$
s	$4.163\ 151\ 291\ 774\ 389\ 6 \times 10^2$	s^2	$-3.140\ 435\ 779\ 506\ 947 \times 10^3$
$s\ \tau$	$-1.269\ 410\ 018\ 182\ 362 \times 10^4$	$s^{2.5}$	$2.975\ 170\ 149\ 976\ 973 \times 10^3$
$s\ \tau^2$	$4.405\ 718\ 471\ 829\ 68 \times 10^3$	s^3	$-1.760\ 137\ 081\ 144\ 729 \times 10^3$
$s\ \tau^3$	$-2.132\ 969\ 018\ 502\ 641\ 6 \times 10^3$	$s^{3.5}$	$4.145\ 655\ 751\ 783\ 703 \times 10^2$

dbar. Another check value is $\rho = 1017.842\ 890\ 411\ 98\ \text{kg m}^{-3}$, corresponding to $S = 20$ psu, $\Theta = 20^\circ\text{C}$ (where $\theta = 19.556\ 279\ 071\ 134\ 4^\circ\text{C}$), and $p = 1000$ dbar. Over the very large (S - Θ - p) cube $[0, 50\ \text{psu}] \times [-10^\circ\text{C}, 50^\circ\text{C}] \times [0\ \text{dbar}, 10^4\ \text{dbar}]$, $P_n(S, \Theta, p)$ and $P_d(S, \Theta, p)$ are stable, exhibiting no potential zeros; $P_n(S, \Theta, p)$ varies from 925 to nearly 1620, while $P_d(S, \Theta, p)$ varies from 0.92 to just under 1.6. Note that the evaluation of potential density referred to pressure p_r is simply $\rho(S, \Theta, p_r)$ for a water parcel with salinity S and conservative temperature Θ .

c. The $\theta(S, \Theta)$ inverse function

The algorithm for finding potential temperature θ from salinity S and conservative temperature Θ , namely, $\theta = \theta(S, \Theta)$, follows from the solution of the nonlinear equation

$$\Theta(S, \theta) = \Theta \tag{B6}$$

for θ . Conservative temperature $\Theta(S, \theta)$ is defined directly in terms of the enthalpy polynomial derived from the F03 Gibbs function [see Eq. (B1)]. The solution of (B6) is found using a modified Newton-Raphson technique, very similar to the procedure used to compute potential temperature θ from salinity S , in situ temperature T , pressure p , and the reference pressure p_r , as described in the first subsection of appendix A above.

We again begin with a simple rational function approximation for θ as a function of S and Θ , given a first estimate of potential temperature θ_0 , as

$$\theta_0(S, \Theta) = P_n(S, \Theta)/P_d(S, \Theta), \tag{B7}$$

where $P_n(S, \Theta)$ and $P_d(S, \Theta)$ are polynomials as defined in Table B3. These coefficients were obtained by fitting the rational function to (S, θ, Θ) triples generated from 10^4 uniformly chosen points in the $S - \theta$ plane $0 \leq S \leq 42$ psu, $-2^\circ\text{C} \leq \theta \leq 40^\circ\text{C}$. Elimination of three of the coefficients by writing them in terms of other unknown coefficients results in the rational func-

TABLE B2. Terms and coefficients of the polynomials $P_n(S, \Theta, p)$ and $P_d(S, \Theta, p)$ that define the rational function equation of state [Eq. (B5)].

$P_n(S, \Theta, p)$	Coefficients	$P_d(S, \Theta, p)$	Coefficients
Constant	$9.998\ 391\ 287\ 877\ 144\ 6 \times 10^2$	Constant	1.0
Θ	$7.068\ 713\ 352\ 265\ 289\ 6 \times 10^0$	Θ	$7.005\ 166\ 573\ 967\ 229\ 8 \times 10^{-3}$
Θ^2	$-2.274\ 684\ 191\ 623\ 296\ 5 \times 10^{-2}$	Θ^2	$-1.504\ 080\ 410\ 737\ 701\ 6 \times 10^{-5}$
Θ^3	$5.656\ 911\ 486\ 140\ 012\ 1 \times 10^{-4}$	Θ^3	$5.394\ 391\ 528\ 842\ 671\ 5 \times 10^{-7}$
S	$2.384\ 997\ 595\ 259\ 334\ 5 \times 10^0$	Θ^4	$3.381\ 160\ 042\ 708\ 341\ 4 \times 10^{-10}$
$S\Theta$	$3.176\ 192\ 431\ 486\ 700\ 9 \times 10^{-4}$	S	$1.559\ 950\ 704\ 615\ 376\ 9 \times 10^{-3}$
S^2	$1.745\ 905\ 301\ 054\ 796\ 2 \times 10^{-3}$	$S\Theta$	$-1.813\ 735\ 246\ 650\ 051\ 7 \times 10^{-6}$
p	$1.219\ 253\ 631\ 017\ 377\ 6 \times 10^{-2}$	$S\Theta^3$	$-3.358\ 015\ 876\ 333\ 536\ 7 \times 10^{-10}$
$p\Theta^2$	$2.464\ 343\ 573\ 166\ 394\ 9 \times 10^{-7}$	$S^{3/2}$	$5.714\ 999\ 759\ 756\ 109\ 9 \times 10^{-6}$
pS	$4.052\ 540\ 533\ 279\ 488\ 8 \times 10^{-6}$	$S^{3/2}\Theta^2$	$7.802\ 587\ 397\ 810\ 737\ 5 \times 10^{-10}$
p^2	$-2.389\ 083\ 130\ 911\ 318\ 7 \times 10^{-8}$	p	$7.103\ 805\ 287\ 252\ 284\ 4 \times 10^{-6}$
$p^2\Theta^2$	$-5.901\ 618\ 247\ 119\ 689\ 1 \times 10^{-12}$	$p^2\Theta^3$	$-2.169\ 230\ 173\ 946\ 009\ 4 \times 10^{-17}$
		$p^3\Theta$	$-8.256\ 408\ 001\ 645\ 856\ 0 \times 10^{-18}$

TABLE B3. Terms and coefficients of the polynomials $P_n(S, \Theta)$ and $P_d(S, \Theta)$ that define the rational function estimate $\theta_0(S, \Theta)$ according to (B7).

$P_n(S, \Theta)$	Coefficients	$P_d(S, \Theta)$	Coefficients
Constant	$-1.446\ 013\ 646\ 344\ 788 \times 10^{-2}$	Constant	1.0
Θ	$9.477\ 566\ 673\ 794\ 488 \times 10^{-1}$	Θ	$3.830\ 289\ 486\ 850\ 898 \times 10^{-3}$
Θ^2	$3.828\ 842\ 955\ 039\ 902 \times 10^{-3}$	Θ^2	$1.247\ 811\ 760\ 368\ 034 \times 10^{-6}$
S	$-3.305\ 308\ 995\ 852\ 924 \times 10^{-3}$	S	$6.506\ 097\ 115\ 635\ 800 \times 10^{-4}$
$S\Theta$	$2.166\ 591\ 947\ 736\ 613 \times 10^{-3}$		
S^2	$1.062\ 415\ 929\ 128\ 982 \times 10^{-4}$		

tion exactly satisfying $\theta_0(0, 0) = -1.446\ 013\ 646\ 344\ 788 \times 10^{-2}$ °C, $\theta_0(35\ \text{psu}, 0) = 0^\circ\text{C}$, and $\theta_0(35\ \text{psu}, 25) = 25^\circ\text{C}$. The nonzero value for $\theta_0(0, 0)$ follows from the fact that enthalpy in F03 is nonzero at ($S = 0, T = 0, p = 0$), unlike enthalpy in FH95.

We now use this rational function as the starting estimate of θ for one iteration of the classic Newton–Raphson technique:

$$\theta = \theta_0 - (\Theta(S, \theta_0) - \Theta)/\Theta_\theta(S, \theta_0). \quad (\text{B8})$$

The derivative Θ_θ can be obtained from the heat capacity at the reference pressure since

$$\Theta_\theta(S, \theta) = C_p(S, T = \theta, p = 0)/C_p^0. \quad (\text{B9})$$

The heat capacity C_p is found by differentiating the Gibbs function $g(S, T, p)$ of F03 according to the standard thermodynamic expression

$$\begin{aligned} C_p(S, T, p) &= \partial h / \partial T|_{S,p} \\ &= -(273.15K + T)\partial^2 g(S, T, p) / \partial T^2 \end{aligned} \quad (\text{B10})$$

where T is in situ (Celsius) temperature.

Check values for θ are $\theta(S = 20\ \text{psu}, \Theta = 20^\circ\text{C}) = 19.556\ 279\ 106\ 043\ 6^\circ\text{C}$,

$$\begin{aligned} \theta(0\ \text{psu}, 0^\circ\text{C}) &= -0.014\ 460\ 136\ 463\ 447\ 9^\circ\text{C}, \\ \theta(35\ \text{psu}, 0^\circ\text{C}) &= 0^\circ\text{C}, \quad \text{and} \quad \theta(35\ \text{psu}, 25^\circ\text{C}) = 25^\circ\text{C}. \end{aligned}$$

APPENDIX C

Rational Function Expressions for the Freezing Temperature

The freezing temperature $T_f(S, p)$ of seawater is taken (as in F03 and FW05) as that temperature T_f for which the chemical potentials of water in seawater and ice, $\mu^W(S, T, p)$ and $\mu^I(T, p)$ coincide. That is, T_f satisfies

$$\mu^W(S, T_f, p) = \mu^I(T_f, p). \quad (\text{C1})$$

The two chemical potentials are given explicitly as

$$\mu^W(S, T, p) = g(S, T, p) - S\partial g / \partial S|_{T,p}; \quad (\text{C2})$$

$$\mu^I(T, p) = g^I(T, p), \quad (\text{C3})$$

where $g(S, T, p)$ and $g^I(T, p)$ are the Gibbs potentials for seawater and ice, respectively. The corresponding parameter values for defining $g(S, T, p)$ and $g^I(T, p)$ are taken from F03 and FW05. Freezing point data can then be computed as the fixed points of a Newton–Raphson iterative solution of (C1)–(C3).

The rational functions we use to approximate the freezing points of seawater are

$$T_f(S, p) = \frac{P_n^T(S, p)}{P_d^T(S, p)}, \quad \theta_f(S, p) = \frac{P_n^\theta(S, p)}{P_d^\theta(S, p)}, \quad \Theta_f(S, p) = \frac{P_n^\Theta(S, p)}{P_d^\Theta(S, p)}, \quad (\text{C4})$$

where the six polynomials $P_n^T(S, p)$, $P_d^T(S, p)$, $P_n^\theta(S, p)$, $P_d^\theta(S, p)$, $P_n^\Theta(S, p)$, and $P_d^\Theta(S, p)$ are defined in Table C1. Here $\theta_f(S, p)$ and $\Theta_f(S, p)$ are, respectively, the potential (with respect to $p_r = 0$ dbar) and conservative temperatures corresponding to the freezing in situ temperature $T_f(S, p)$. The forms of these functions were chosen so that the numbers of terms required were as small as possible while still achieving rms fitting accuracies at least as good as those obtained in F03, viz. 1.5 mK. We also tried to minimize the differences in forms between the three rational functions; the forms for potential and conservative temperature, in fact, being identical and the form for in situ temperature differing from these by only one term in the numerator. The constant in the numerator for each temperature variable was assigned its value so that $T_f(0\ \text{psu}, 0\ \text{dbar}) = \theta_f(0\ \text{psu}, 0\ \text{dbar}) = 2.518\ 051\ 674\ 454\ 129 \times 10^{-3}$ °C and $\Theta_f(0\ \text{psu}, 0\ \text{dbar}) = 1.794\ 500\ 432\ 452\ 963 \times 10^{-2}$ °C were the solutions of (C1)–(C3) precisely, while the other values in the table were computed from least squares fits to 10^4 uniformly distributed points in (S, p) space inside the rectangle $[0, 42\ \text{psu}] \times [0\ \text{dbar}, 5000\ \text{dbar}]$. Check values for the freezing temperatures are

TABLE C1. Coefficients of the 11-term rational functions (C4) for the freezing temperatures of seawater.

Terms	$P_n^T(S, p)$ coefficients	$P_d^T(S, p)$ coefficients
Constant	$2.518\ 051\ 674\ 454\ 129\ 0 \times 10^{-3}$	1.0
S	$-5.894\ 666\ 954\ 857\ 631\ 0 \times 10^{-2}$	
$S^{1.5}$	$2.481\ 142\ 231\ 911\ 077\ 6 \times 10^{-3}$	
S^2	$-3.193\ 009\ 163\ 149\ 609\ 8 \times 10^{-4}$	
$S^{2.5}$		$-4.330\ 156\ 812\ 699\ 863\ 0 \times 10^{-7}$
S^4	$1.563\ 717\ 414\ 395\ 548\ 5 \times 10^{-8}$	
p	$-7.427\ 696\ 181\ 481\ 005\ 3 \times 10^{-4}$	$-1.962\ 551\ 878\ 683\ 189\ 0 \times 10^{-6}$
p^2	$-1.431\ 221\ 659\ 622\ 791\ 8 \times 10^{-8}$	$7.058\ 856\ 506\ 481\ 658\ 4 \times 10^{-11}$
Terms	$P_n^0(S, p)$ coefficients	$P_d^0(S, p)$ coefficients
Constant	$2.518\ 051\ 674\ 454\ 129\ 0 \times 10^{-3}$	1.0
S	$-5.854\ 586\ 369\ 892\ 618\ 4 \times 10^{-2}$	
$S^{1.5}$	$2.297\ 998\ 578\ 012\ 432\ 5 \times 10^{-3}$	
S^2	$-3.008\ 633\ 821\ 823\ 550\ 0 \times 10^{-4}$	
$S^{2.5}$		$1.363\ 248\ 194\ 428\ 590\ 9 \times 10^{-6}$
p	$-7.002\ 353\ 002\ 935\ 180\ 3 \times 10^{-4}$	$-3.849\ 326\ 630\ 917\ 207\ 4 \times 10^{-5}$
p^2	$8.414\ 960\ 721\ 983\ 380\ 6 \times 10^{-9}$	$9.168\ 653\ 744\ 674\ 964\ 1 \times 10^{-10}$
Sp^2	$1.184\ 585\ 756\ 310\ 740\ 3 \times 10^{-11}$	
Terms	$P_n^0(S, p)$ coefficients	$P_d^0(S, p)$ coefficients
Constant	$1.794\ 500\ 432\ 452\ 963\ 0 \times 10^{-2}$	1.0
S	$-5.840\ 358\ 459\ 168\ 866\ 5 \times 10^{-2}$	
$S^{1.5}$	$2.457\ 326\ 870\ 423\ 775\ 7 \times 10^{-3}$	
S^2	$-3.432\ 791\ 911\ 465\ 858\ 6 \times 10^{-4}$	
$S^{2.5}$		$1.471\ 968\ 039\ 552\ 875\ 8 \times 10^{-6}$
p	$-7.398\ 125\ 503\ 799\ 030\ 7 \times 10^{-4}$	$-1.750\ 942\ 102\ 705\ 495\ 4 \times 10^{-5}$
p^2	$-7.384\ 503\ 446\ 750\ 393\ 0 \times 10^{-9}$	$5.215\ 309\ 581\ 272\ 078\ 7 \times 10^{-10}$
Sp^2	$1.906\ 979\ 390\ 293\ 770\ 8 \times 10^{-11}$	

$$T_f(35 \text{ psu}, 200 \text{ dbar}) = -2.070\ 973\ 701\ 805\ 972^\circ\text{C},$$

$$\theta_f(35 \text{ psu}, 200 \text{ dbar}) = -2.074\ 408\ 175\ 943\ 127^\circ\text{C},$$

$$\Theta_f(35 \text{ psu}, 200 \text{ db}) = -2.071\ 222\ 603\ 621\ 528^\circ\text{C}.$$

All of the freezing points of seawater defined by (C4), as well as the freezing points in F03 and FW05 defined by the solutions of (C1)–(C3) above, refer to air-free water. Seawater is typically air saturated, in which case we follow F03 in applying a small correction to these air-free freezing points to obtain freezing points of seawater saturated with air. For in situ temperature and potential temperature (since $\partial\theta/\partial T = 1$ at $p = p_f = 0$), the linear salinity offset of Eq. (66) of F03 gives freezing points for saturated seawater as

$$T_f^{\text{sat}}(S, p) = T_f(S, p) - 2.518\ 051\ 674\ 454\ 129 \text{ mK} \\ + \frac{S}{35} 0.5 \text{ mK} \quad (\text{C5a})$$

and

$$\theta_f^{\text{sat}}(S, p) = \theta_f(S, p) - 2.518\ 051\ 674\ 454\ 129 \text{ mK} \\ + \frac{S}{35} 0.5 \text{ mK}. \quad (\text{C5b})$$

The constant here is different from the 2.4 mK of F03, but agrees with the currently best normal pressure freezing point of pure air-free water $T_f = 0.002\ 518 \pm 0.000\ 002^\circ\text{C}$ given in FW05 and was chosen so that $T_f^{\text{sat}}(0, 0) = \theta_f^{\text{sat}}(0, 0) = 0$ exactly. Note, however, that the Celsius zero point $T_f^{\text{sat}}(0, 0) = \theta_f^{\text{sat}}(0, 0) = 0^\circ\text{C}$ (i.e., 273.15 K) is deliberately defined by the ITS-90 specification (Preston-Thomas 1990) but is not necessarily the best known value for the freezing point of air-saturated freshwater at atmospheric pressure. For conservative temperature we adopt a similar linear salinity correction where the constant and linear coefficient have been found by ensuring that $\Theta_f^{\text{sat}}(S = 0, p = 0)$ is equal to $\Theta(S = 0, \theta = \theta_f^{\text{sat}}(S = 0, p = 0)) = \Theta(0, 0)$ and also that $\Theta_f^{\text{sat}}(35 \text{ psu}, 0 \text{ dbar}) = \Theta(35, \theta_f^{\text{sat}}(35 \text{ psu}, 0 \text{ dbar}))$. This yields the following expression for the freezing conservative temperature of seawater that is saturated with air:

$$\Theta_f^{\text{sat}}(S, p) = \Theta_f(S, p) - 2.661\ 425\ 530\ 980\ 574 \text{ mK} \\ + \frac{S}{35} 0.660\ 596\ 597\ 408\ 344\ 4 \text{ mK}, \quad (\text{C5c})$$

TABLE C2. Coefficients of simple approximate three-term linear functions for freezing temperatures, each designed so that if the temperature of a seawater parcel exceeds this approximate expression, then the parcel is definitely above the freezing temperature.

Term	$T_f^{\text{sat}}(S, p)$	$\theta_f^{\text{sat}}(S, p)$	$\Theta_f^{\text{sat}}(S, p)$
Constant ($^{\circ}\text{C}$)	1.33×10^{-1}	3.09×10^{-1}	1.99×10^{-1}
S (psu)	-5.54×10^{-2}	-6.09×10^{-2}	-5.68×10^{-2}
p (dbar)	-8.27×10^{-4}	-8.51×10^{-4}	-8.56×10^{-4}

Check values for the saturated freezing temperatures of seawater are $T_f^{\text{sat}}(35 \text{ psu}, 200 \text{ dbar}) = -2.072\ 991\ 753\ 480\ 427^{\circ}\text{C}$, $\theta_f^{\text{sat}}(35 \text{ psu}, 200 \text{ dbar}) = -2.076\ 426\ 227\ 617\ 581^{\circ}\text{C}$, and $\Theta_f^{\text{sat}}(35 \text{ psu}, 200 \text{ dbar}) = -2.073\ 223\ 432\ 555\ 101^{\circ}\text{C}$.

Finally, we provide simple linear expressions for upper bounds of the three saturated freezing temperatures of (C5). Ocean models need to know whether the temperature variable that they are carrying is in the vicinity of the corresponding freezing temperature of seawater. Rather than testing temperature against the appropriate temperature formula from (C5), a linear bound will enable an efficient test for determining the state of most of the ocean's volume. Table C2 contains coefficients for these saturated freezing point upper bounds. The coefficients contained in the table have been rounded to two decimal places, in the appropriate direction, so that seawater with a temperature larger than the bound will definitely be in the liquid state. Failing this linear test will then require use of the more complicated formulas in (C5) and (C4) to determine the state of a seawater parcel.

REFERENCES

- Bradshaw, A., and K. E. Schleicher, 1970: Direct measurements of thermal expansion of sea water under pressure. *Deep-Sea Res.*, **17**, 691–706.
- Brewer, P. G., and A. Bradshaw, 1975: The effect of the non-ideal composition of sea water on salinity and density. *J. Mar. Res.*, **33**, 157–175.
- Caldwell, D. R., 1978: The maximum density points of pure and saline water. *Deep-Sea Res.*, **25**, 175–181.
- Culkin, F., 1965: The major constituents of seawater. *Chemical Oceanography*, J. P. Riley and G. Skirrow, Eds., Vol. 1, Academic Press, 72–120.
- Doherty, B. T., and D. R. Kester, 1974: Freezing point of seawater. *J. Mar. Res.*, **23**, 285–300.
- Dorsey, N. E., 1968: *Properties of Ordinary Water-Substance in All Its Phases: Water-Vapor, Water, and All the Ices*. Hafner Publishing Company, 657 pp.
- Feistel, R., 2003: A new extended Gibbs thermodynamic potential of seawater. *Progress in Oceanography*, Vol. 58, Pergamon Press, 43–114.
- , 2004: A new extended Gibbs thermodynamic potential of seawater. *Progress in Oceanography*, Vol. 58, Pergamon, 43–114; *Corrigendum*, Vol. 61, Pergamon Press, 99.
- , and E. Hagen, 1995: On the GIBBS thermodynamic potential of seawater. *Progress in Oceanography*, Vol. 36, Pergamon Press, 249–327.
- , and —, 1998: A Gibbs thermodynamic potential of sea ice. *Cold Reg. Sci. Technol.*, **28**, 83–142.
- , and W. Wagner, 2005: High-pressure thermodynamic GIBBS function of ice and sea ice. *J. Mar. Res.*, **63**, 95–139.
- Fofonoff, N. P., 1985: Physical properties of seawater: A new salinity scale and equation of state for seawater. *J. Geophys. Res.*, **90**, 3332–3342.
- , 1992: *Physical oceanography*. Earth and Planetary Physics Lecture Notes 226, Harvard University, 66 pp.
- , and R. C. Millard, 1983: Algorithms for computation of fundamental properties of seawater. UNESCO Tech. Papers in Marine Science 44, UNESCO, 53 pp.
- Fujino, R., E. L. Lewis, and R. G. Perkin, 1974: The freezing point of seawater at pressures up to 100 bars. *J. Geophys. Res.*, **79**, 1792–1797.
- Gouretski, V. V., and K. P. Koltermann, 2004: WOCE global hydrographic climatology. *Berichte des Bundesamtes für Seeschifffahrt und Hydrographie Tech. Rep.* 35, 49 pp.
- Gradshteyn, I. S., and I. M. Ryzhik, 1980: *Tables of Integrals, Series and Products*. Academic Press, 1160 pp.
- Henderson, S. J., and R. J. Speedy, 1987: Melting temperature of ice at positive and negative pressures. *J. Phys. Chem.*, **91**, 3069–3072.
- Koltermann, K. P., V. Gouretski, and K. Jancke, 2004: *Atlantic Ocean*. Vol. 4, *Hydrographic Atlas of the World Ocean Circulation Experiment (WOCE)*, International WOCE Project Office. [Available online at www.bsh.de/aktat/mk/AIMS.]
- Landau, L. D., and E. M. Lifshitz, 1959: *Fluid Mechanics*. Pergamon, 536 pp.
- Lewis, E. L., and R. G. Perkin, 1981: The practical salinity scale 1978: Conversion of existing data. *Deep-Sea Res.*, **28A**, 307–328.
- McDougall, T. J., 1987: Thermobaricity, cabbeling, and water-mass conversion. *J. Geophys. Res.*, **92**, 5448–5464.
- , 2003: Potential enthalpy: A conservative oceanic variable for evaluating heat content and heat fluxes. *J. Phys. Oceanogr.*, **33**, 945–963.
- , and R. Feistel, 2003: What causes the adiabatic lapse rate? *Deep-Sea Res.*, **50A**, 1523–1535.
- , D. R. Jackett, D. G. Wright, and R. Feistel, 2003: Accurate and computationally efficient algorithms for potential temperature and density of seawater. *J. Atmos. Oceanic Technol.*, **20**, 730–741.
- Millero, F. J., 1978: Freezing point of seawater. UNESCO Tech. Papers in Marine Science 28, 35 pp.
- , 1982: The thermodynamics of seawater. Part 1. The PVT properties. *Ocean Sci. Eng.*, **7**, 403–460.
- , 2000: Effect of changes in the composition of seawater on the density-salinity relationship. *Deep-Sea Res.*, **47A**, 1583–1590.
- , and W. H. Leung, 1976: The thermodynamics of seawater at one atmosphere. *Amer. J. Sci.*, **276**, 1035–1077.
- Preston-Thomas, H., 1990: The international temperature scale of 1990 (ITS-90). *Metrologia*, **27**, 3–10.
- Wagner, W., and A. Pruß, 2002: The IAPWS Formulation 1995 for the thermodynamic properties of ordinary water substance for general and scientific use. *J. Phys. Chem. Ref. Data*, **31**, 387–535.
- Yen, Y.-C., 1981: Review of the thermal properties of snow, ice and sea ice. Cold Regions Research and Engineering Laboratory Rep. 81-10, 27 pp.